Auton Robot (2010) 28: 331–353
DOI 10.1007/s10514-009-9172-5

Integration of posture and rhythmic motion controls in quadrupedal dynamic walking using phase modulations based on leg loading/unloading

Christophe Maufroy · Hiroshi Kimura · Kunikatsu Takase

Received: 23 April 2009 / Accepted: 17 December 2009 / Published online: 9 February 2010

Abstract In this paper, we intend to show the basis of a general legged locomotion controller with the ability to integrate both posture and rhythmic motion controls and shift continuously from one control method to the other according to the walking speed. The rhythmic motion of each leg in the sagittal plane is generated by a single leg controller which controls the swing-to-stance and stance-to-swing phase transitions using respectively leg loading and unloading information. Since rolling motion induced by inverted pendulum motion during the two-legged stance phases results in the transfer of the load between the contralateral legs, leg loading/unloading involves posture information in the frontal plane. As a result of the phase modulations based on leg loading/unloading, rhythmic motion of each leg is achieved and inter-leg coordination (resulting in a gait) emerges, even without explicit coordination amongst the leg controllers, allowing to realize dynamic walking in the low- to medium-speed range. We show that the proposed method has resistance ability against lateral perturbations to some extent, but that an additional ascending coordination mechanism between ipsilateral legs is necessary to withstand perturbations decreasing the rolling motion amplitude. Even without stepping reflex using vestibular information, our control system, relying on phase modulations based on leg loading/unloading and the ascending coordination mechanism between ipsilateral legs, enables low speed dynamic walking on uneven terrain with long cyclic period, which was not realized in our former studies. Details of trajectory generation, movies of simulations and movies of preliminary experiments using a real robot are available at: http://robotics.mech.kit.ac.jp/kotetsu/.

Keywords Quadrupedal walking · Central pattern generator · Phase modulations · Leg loading/unloading · Gait and posture · Perturbations

C. Maufroy (✉)
Locomotion Laboratory, Friedrich-Schiller University Jena, Jena, Germany
e-mail: christophe.maufroy@uni-jena.de

C. Maufroy
Division of Mechanical and System Engineering, Kyoto Institute of Technology, Kyoto, Japan

H. Kimura
Graduate School of Science and Technology, Kyoto Institute of Technology, Kyoto, Japan
e-mail: kimura@mech.kit.ac.jp

K. Takase
Graduate School of Information Systems, University of Electro-Communications, Tokyo, Japan
e-mail: takase@is.uec.ac.jp

1 Introduction

Animals are able of great mobility, while taking advantage of the dynamics of their bodies and environment such as the gravity field, the hydrodynamic field and so on. Regarding legged locomotion, Alexander (1984, 1992) showed that the Froude Number[1] (Fr) can be used to characterize the dynamical phenomena taking place when the locomotion speed varies. It was also pointed out by Fukuoka et al. (2003) that:

[1] $Fr = v/\sqrt{gh}$ (where v is the locomotion speed, g the gravity acceleration and h the height of the hip joint from the ground).

- At low *Fr* (low speed), since potential energy is dominant, posture[2] control using ground reaction force information and vestibular information is predominant to generate stable locomotion.
- At high *Fr* (high speed), since kinetic energy is dominant, it requires rhythmic motion[3] control to maintain the stable limit-cycle[4] which results from the non-linear dynamics of the combined control and mechanical systems. Posture control using vestibular information (such as the stepping reflex) is also involved to stabilize the system when its state leaves the limit-cycle stable region due to perturbations.

In walking at low *Fr* of biped robots (Takanishi et al. 1990; Hirai et al. 1998) and of a quadruped robot (Yoneda et al. 1994), stabilization of posture and rhythmic motion at low speed was realized by joint PD-control to follow joint reference trajectories satisfying constraints on the ZMP,[5] in order to preserve the "dynamic balance" at each instant during the gait (Vukobratović and Borovac 2004). In such ZMP-based control method, posture and rhythmic motion controls are integrated in some sense (Fig. 1(a): right), but energy efficiency decreases as the walking speed increases, since a body with a large mass needs to be accelerated and decelerated by the actuators in every step cycle to satisfy the ZMP constraints.

On the other hand, in walking at medium *Fr* and in running at high *Fr*, stable limit-cycle patterns were constructed by the rhythmic exchange of stance and swing phases, while posture control such as touchdown angle control based on vestibular information (or *stepping reflex*) also contributed to stabilization of the limit-cycle patterns (Fig. 1(a): left) (Miura and Shimoyama 1984; Raibert 1986; Kimura et al. 1990). Hence, limit-cycle-based control methods are not bound to preserve the "dynamic balance" at each instant of the gait and this creates more freedom to optimize energy efficiency (Hobbelen and Wisse 2008) by taking advantage of the natural dynamics of the system (related to inverted pendulum mode or spring-mass mode). As a result, such methods can generate more energy efficient middle- and high-speed locomotion than ZMP-based control methods. However, there is an upper limit to the cyclic period, over which stable dynamic walking cannot be realized with such type of control (Kimura et al. 1990; Aoi and Tsuchiya 2006), which limits its use to generate low speed locomotion.

In this paper, we consider a limit-cycle-based control method for quadrupedal dynamic walking of a medium-sized mammal-like model. Quadrupedal mammals usually have long and narrow bodies and contralateral legs are never simultaneously in the swing phase during walking. Therefore, posture in the sagittal plane is easy to stabilize, and the main issue is to control the posture in the frontal plane, that is, to stabilize the rolling motion of the body (Karayannidou et al. 2009). In the author's former studies (Fukuoka et al. 2003; Kimura and Fukuoka 2004; Kimura et al. 2007), adaptive walking on irregular terrain with the mammal-like quadruped robot *Tekken* was realized in the medium-speed range ($Fr \in [0.3, 0.7]$), using a biologically-inspired control system based on a Central Pattern Generator (CPG) associated with a set of reflexes. In animals, CPGs are neural circuits responsible for the generation of rhythmic movements, including locomotion (Grillner 1981). In those studies, rolling motion feedback to the CPG and sideway stepping reflexes based on vestibular information (roll angle of the body) were employed to control the posture in the frontal plane. However, stable low speed walking (with $Fr < 0.3$) with a long cyclic period (>0.6 s) could not be realized.[6] This was because ground reaction force (reflecting the load supported by each leg, or *leg loading*) sensory feedback to the CPG for posture control was lacking and the large amplitude of the rolling motion induced by the long cyclic period made walking unstable.

On the other hand, in four-legged mammals, posture control is known to be mainly based on somatosensory input, in particular sensory information related to leg loading provided by the Golgi tendon organs (Deliagina and Orlovsky 2002). In addition, recent simulation studies also indicated that this sensory information is crucial for the coordination of contralateral legs during walking (Ekeberg and Pearson 2005). Therefore, we propose a novel control method for quadrupedal dynamic walking, using leg loading/unloading information to adjust the relative durations of the swing and stance phases of each leg during the step cycle, via phase modulations. As local leg loading/unloading information reflects both the current phasic state of a leg (swing or stance) and the global body posture, such method allows to simultaneously coordinate the rhythmic motion of the legs in the sagittal plane and control the posture of the body in the frontal plane. We show in simulations that such simple but general legged locomotion controller can integrate both posture control and rhythmic motion control in the framework

[2] Posture here refers respectively to the attitude when the body is at rest, and the mean attitude and the amplitude of the body motions (such as the rolling motion) during locomotion.

[3] Rhythmic motion involves periodic motion of each leg and the coordination among the legs (or interleg coordination), resulting in a gait.

[4] A stable limit cycle is a close trajectory in the state-space (i.e. a periodic motion) to which neighboring trajectories converge under small perturbations.

[5] The Zero Moment Point (or ZMP) is the point with respect to which the moment of all the ground reaction forces is zero. It can be seen as the extension of the projection of the center of gravity on the ground, including inertial forces and so on.

[6] Stable low speed walking with the short cyclic period and short strides was realized, but is not good from the energy efficiency point of view.

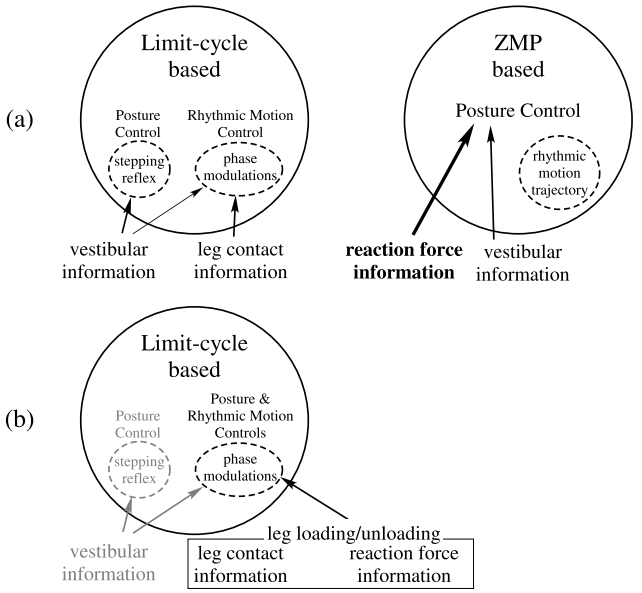

Fig. 1 (**a**) Conventional legged locomotion control methods. In limit-cycle-based control methods, posture control is usually achieved using mechanisms relying on vestibular information (such as the stepping reflex), while control of the rhythmic motion relies on phase modulations based on leg contact information and, to a lesser extent, vestibular information in the case of the rolling motion feedback to the CPG in Tekken (Fukuoka et al. 2003). (**b**) Legged locomotion control method proposed in this paper. We employ an approach where both posture and rhythmic motion controls are achieved using a single mechanism, i.e. phase modulations based on leg loading/unloading information

of limit-cycle-based control (Fig. 1(b)), and that it can generate stable dynamic walking at low and medium *Fr* even under some perturbations, without using vestibular information.

Section 2 presents the related studies and details the approach followed in this study. An overview of the simulation model is given in Sect. 3, while Sect. 4 presents the proposed control system. Our results are presented in Sect. 5. Section 5.1 deals with the issue of interleg coordination and explains how our strategy, relying on phase modulations based on leg loading/unloading, allows to realize stable dynamic walking with independent leg controllers. Section 5.2 investigates the performances of the control system against perturbations (lateral perturbations and uneven terrain) and explains why an ascending coordination between the ipsilateral LCs is needed. We discuss our results in Sect. 6 and finally conclude in Sect. 7.

Abbreviations and notations used in the following sections are summarized in Tables 1 and 2. The hat $\hat{}$, the bar $\bar{}$ and the tilde $\tilde{}$ symbols are respectively used to represent the nominal value, the real value (observed during the simulation) and the reference value of a single variable.

Table 1 Abbreviations

ACM	Ascending coordination mechanism
AEP, PEP	Anterior and posterior extreme positions
CPG	Central pattern generator
LC	Leg controller
LF, RF	Left and right forelegs
LH, RH	Left and right hind legs
LO, TD	Lift off and touch down
ST or st, SW or sw	Stance and swing
cntr, ipsi	Contralateral and ipsilateral

2 Related studies and our approach

2.1 Legged locomotion control methods

Kimura et al. (2007), referring to Jindrich and Full (2002), mentioned that three general methods are available to maintain stability during legged locomotion. Those are:

(a) adjustment of the joint torques within a single step cycle,
(b) adjustment of the initial conditions of the legs at the transition from swing to stance,
(c) adjustment of the phase (stance or swing) of a leg, or *phase modulations*.[7]

Method [a] is very popular in a lot of legged locomotion studies including ZMP-based control. Method [b] involves the adjustment of the touchdown angle of a swinging leg based on vestibular information, or stepping reflex (Miura and Shimoyama 1984; Raibert 1986; Kimura et al. 1990, 2007; Kimura and Fukuoka 2004; Fukuoka et al. 2003), and the switching of leg stiffness between stance and swing phases (Raibert 1986; Kimura et al. 1990, 2007; Kimura and Fukuoka 2004; Taga et al. 1991; Taga 1995; Fukuoka et al. 2003). Method [c] is based on the biological knowledge that rhythmic motion in animals is mainly generated by neural circuits called CPG, whose activity is modulated by sensory inputs (Grillner 1981; Rossignol 1996; Orlovsky et al. 1999). The CPG-based method was used to generate dynamic walking in simulation (Taga et al. 1991; Taga 1995; Ijspeert 2001; Tomita and Yano 2003; Righetti and Ijspeert 2008) and real robots (Kimura et al. 1999, 2007; Kimura and Fukuoka 2004; Berns et al. 1999; Tsujita et al. 2001; Fukuoka et al. 2003; Aoi and Tsuchiya 2005; Buchli and Ijspeert 2008; Ijspeert et al. 2007). The stability of this method has also been analyzed mathematically (Aoi and Tsuchiya 2006). These three methods are of course not

[7] That is, shortening or lengthening the period of the stance or swing phase of a leg in a step cycle.

Table 2 Indexes and notations. The suffix i is omitted when we consider a single leg

Indexes and accents			
i	Leg index (superscript) ∈ {RH, LH, RF, LF}; "*" is used as a wildcard character, replacing either the first letter (to indicate both fore- or hind legs) or the second (to indicate both right or left legs)		
j	Joint index (subscript)	k	Walking cycle index (subscript)
p	Leg phase index (subscript) ∈ {sw, st}	s	Side index (superscript)∈ {R, L}
$\hat{*}$, $\bar{*}$, $\tilde{*}$	represent respectively the nominal value, the real value and the reference value of a single variable		
Physical quantities			
f_n^i	Normal ground reaction force	θ_j^i	Joint angle
θ_{roll}	Body roll angle	Θ	Body rolling motion amplitude
Phase dynamics parameters			
ϕ^i	Oscillator phase	ω^i	Oscillator angular velocity
T_{sw}^i	Swing phase duration	T_{st}^i	Stance phase duration
T	Walking cyclic period	β^i	Duty ratio
χ^i	Force threshold of the stance-to-swing transition condition based on leg unloading (N)		
$\phi_{l_1 \to l_2}^i$	Phase threshold of the transition condition based on the oscillator phase (for the transition from l_1 to l_2)		
Trajectory generation parameters			
$\boldsymbol{r}^i$, $\boldsymbol{v}^i$	Position and speed vectors of the foot in the referential fixed to the trunk and centered at the hip joint ($(*)_x$ and $(*)_y$ refer respectively to the x and y coordinates)		
L^i	Stride length	H^i	Height of the hip joint from the ground
Δ^i	Offset of the AEP vertical coordinate		
Γ_j^i	Joint torque	$K_{Pj,p}^i$, $K_{Dj,p}^i$	PD control gains
c^i	Coefficient used to adjust the PD control gains of the knee and ankle joints during the stance phase		
Gait characterization			
γ^{cntr}	Phase difference between contralateral legs (such as LH and RH)		
γ^{ipsi}	Phase difference between ipsilateral hind leg ad foreleg (such as LH and LF)		
Other notation			
$\langle f \rangle_k$	Average value of variable f during walking cycle k, defined as $\langle f \rangle_k = \frac{\int_{t_{s,k}}^{t_{e,k}} f(t)dt}{(t_{e,k} - t_{s,k})}$, when taking respectively the onset of swing phase of the left hind leg in walking cycle k and $k+1$ as the start ($t_{s,k}$) and end ($t_{e,k}$) boundaries of the walking cycle.		

completely independent. For example, the method [c] becomes more effective when the switching of leg stiffness between stance and swing phases is employed.

In this paper, we utilize a CPG-based method with phase modulations based on leg loading/unloading. In addition, even though the stepping reflex is a very effective posture control method, we do not use it in this study at this stage, since we would like to see the effectiveness of the phase modulations for the posture control in the frontal plane directly.

2.2 CPG architecture and phase modulations based on leg loading/unloading

Tsujita et al. (2001) and Aoi and Tsuchiya (2005, 2006) used leg contact information feedback to the CPG. They proposed to modulate the swing phase duration of a leg by resetting the phase of its associated oscillator to the stance phase when the leg touched the ground, and reported that such phase resetting enhanced the stability against perturbations.

On the other hand, it is known for the stance-to-swing transition in animals that stance phase is indeterminately prolongated as long as the leg loading is over a given threshold (Duysens and Pearson 1980; Orlovsky et al. 1999). Being motivated by this fact, Ekeberg and Pearson (2005) investigated the respective importance of hip extension and leg unloading information for stance termination by simulating 2D alternative stepping of the hind legs in the sagittal plane using a musculoskeletal model of cats. They found that modulation of the stance phase duration using leg unloading plays an essential role in the emergence and stabilization of stable alternate stepping. Maufroy et al. (2008) also simulated similar 2D alternative stepping in the sagit-

tal plane in a wide walking speed range while employing synergies of muscle activation. However, in this paper, we consider 3D walking (involving motion in the sagittal but also the frontal planes) and utilize phase modulations based on leg loading/unloading to control both rhythmic motion in the sagittal plane and posture in the frontal plane. In addition, we decided to use a PD-controlled joint model, instead of a musculoskeletal model, for the sake of simplicity.

Righetti and Ijspeert (2008) used phase modulations based on leg loading/unloading in a generic network of coupled oscillators and simulated 3D quadrupedal locomotion with various gaits (walk, trot, bound and pace). In their architecture, the generation of the gait as well as its stabilization was mostly considered at the level of the oscillators interactions by setting properly the couplings among the leg oscillators. Nevertheless, no specific consideration was given to the exact role of the phase modulations based on leg unloading regarding the issues of rhythmic motion generation in the sagittal plane and postural control in the frontal plane. Alternative stepping of the contralateral legs can be generated without explicit couplings among the leg controllers when phase modulations based on leg unloading are used, as shown by Ekeberg and Pearson (2005). Hence, in this paper, we aim at achieving interleg coordination in 3D walking in an emergent fashion, through a process involving interactions with the rolling motion in the frontal plane relayed by leg loading/unloading information, rather than by explicit couplings among the leg control entities. Such CPG architecture is also motivated by the fact that the locomotion CPG in vertebrates is distributed (Rossignol 1996) and the argument by Cruse (2002) that "local rules exploiting feedback loops and the mechanical properties of the body can produce the basic rhythm and can explain a considerable part of the coordination." Using such architecture, we might be able to integrate posture and rhythmic motion controls in a more sensor-dependent way in order to generate appropriate interleg coordination according to the walking speed, hence realizing walking both at low and medium speeds using the same control system.

3 Simulation model

3.1 Mechanical model

Our model (Fig. 2) is made of a trunk and four identical legs, each of them made of three segments (thigh, shank and foot) articulated with three rotational joints around the pitch axis (hip, knee and ankle). At the tip of each foot is a force sensor to measure the normal ground reaction force f_n. The trunk is modeled as a cylindrical body, whose center of mass is slightly forward (at a position of 40% of its length from the front) to account for a similar mass repartition in animals (Tomita 1967). The distances between the hip joints of the contralateral and ipsilateral legs are 12 cm and 23 cm, respectively.

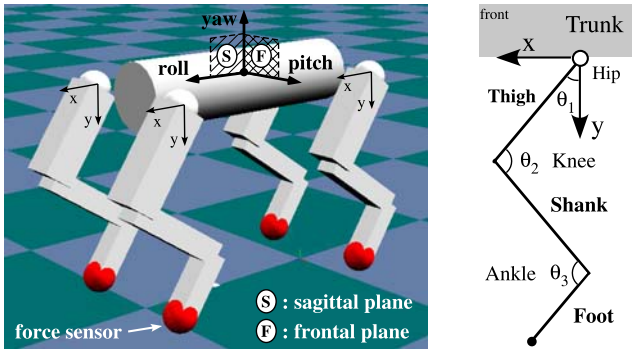

	Length (cm)	Width (cm)	Height (cm)	Mass (g)
Thigh	9	3	3	202.5
Shank	10	2	2	100
Foot	6	2	2	60
	Length (cm)	Radius (cm)		Mass (g)
Trunk	23	3		3000
	Radius (cm)			Mass (g)
Sensor	1.5			50

Fig. 2 Simulation model. Each leg has three segments articulated with three rotational joints around the pitch axis. The model does not include any joint around the roll axis. The masses and dimensions of the model bodies are given in the lower table. They are loosely inspired from the ones of medium-sized mammals such as cats and small dogs (with the forelegs identical to the hind legs). The total mass is 4.650 kg, while the distances between the hip joints of the contralateral and ipsilateral legs are 12 cm and 23 cm, respectively

The legs have no joint around the roll axis so that the motion of each leg is two-dimensional and restricted to a plane parallel to the sagittal plane. But during dynamic walking, rolling motion in the frontal plane with the roll angle represented by θ_{roll} is still naturally induced as a consequence of the rhythmic pitching motion of the legs because a dynamic system similar to an inverted pendulum appears in two-legged stance phases. We employ such mechanical model in order to investigate the effectiveness of phase modulations based on leg loading/unloading for posture control in the frontal plane.

3.2 Simulation environment

The simulations were carried out using a commercial mobile robot simulation software: Webots.[8] The simulation of the mechanical system dynamics (including the computation of the torques generated by the PD control for each joint) was performed every 0.5 ms, while the time step for the

[8] http://www.cyberbotics.com.

simulation of the control system (phase dynamics and trajectory generation) was set to 2 ms. For the ground reaction forces, the contact model provided by ODE (the dynamics engine on which Webots is based) was used. For the normal force component, it is equivalent to a spring-damper model (the parameters were set to realize stiffness and damping respectively equal to 3.0e4 Nm^{-1} and 2.0e3 Nsm^{-1}). On the other hand, the frictional forces in the tangential directions were computed using Coulomb friction approximation (with a friction coefficient set to 1.0).

4 Control system

4.1 Overview

Our control system is based on the Central Pattern Generator (CPG) paradigm and each of the four legs is associated with a control entity that will be referred to as *leg controller* (LC). Each LC has two phases, *swing* (*sw*) and *stance* (*st*), and the transfer of activity between them is regulated using sensory information related to the load supported by the leg, or *leg loading*, as explained in Sect. 4.2.

In order to keep the system simple, as few interleg coordination mechanisms as possible were introduced. While using the phase modulations based on leg loading in the LCs, walk gait could be realized in a broad range of walking speeds and periods without any interleg coordination mechanism (see Sect. 5.1). However, when the model was subjected to perturbations, we found that an interleg control mechanism was necessary and we named it: *ascending coordination mechanism* (or *ACM*), as it links the hind legs to the forelegs. Although it is only used in Sect. 5.2.2 and 5.2.3, it is presented in this section (Sect. 4.3) for the sake of clarity.

4.2 Single leg controller

The internal organization of the LC is schematically represented in Fig. 3, using (1)∼(13). Each LC is associated with a simple oscillator, with a constant and unitary amplitude and a variable phase ϕ^i, where i is the leg index (Tsujita et al. 2001; Aoi and Tsuchiya 2005, 2006). Such representation involving an oscillator was introduced for the sake of simplicity, in order to facilitate the trajectory generation process and the definition of phase relationships between the legs. However, as the phase transitions are regulated using sensory feedback, this latter has a large influence on the locomotion rhythm.

The trajectory of the foot is generated according to the current locomotion phase. For that purpose, a few specific positions need to be defined. The position of the foot where the swing-to-stance transition is desired to happen is called the *anterior extreme position* $\hat{\boldsymbol{r}}_{AEP}$, while the position where it really happens is the *touchdown position* $\boldsymbol{r}_{TD}$. Similarly, the position where the stance-to-swing transition is desired

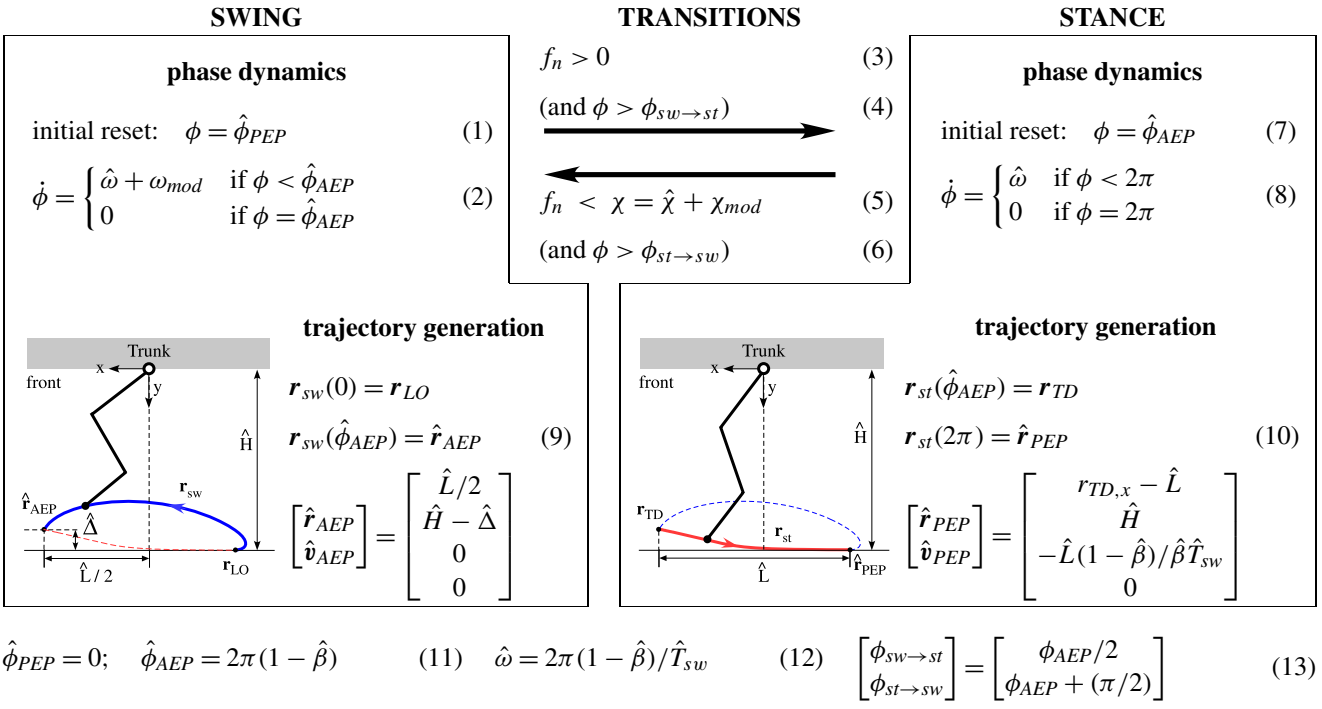

Fig. 3 Leg Controller structure. The foot trajectories are expressed in the Cartesian coordinate system fixed to the trunk and centered at the hip joint ($*_x$ and $*_y$ refer respectively to the x and y coordinates, while $\boldsymbol{r}$ and $\boldsymbol{v}$ are the position and the speed vectors)

to happen is the *posterior extreme position* $\hat{\boldsymbol{r}}_{PEP}$, while the position where it really happens is the *liftoff position* $\boldsymbol{r}_{LO}$.

Constant parameter values of a LC used in the simulations are summarized in Appendix.

4.2.1 Phase dynamics

When a leg phase transition occurs in a LC, ϕ is reset (to $\hat{\phi}_{PEP}$ at the swing onset (1) or to $\hat{\phi}_{AEP}$ at the stance onset (7)). The phase then increases constantly with a rate given by the angular velocity $\hat{\omega}$, until it reaches a maximum value (as expressed by (2) and (8)). The parameter ω_{mod} in (2) is used only by the ascending coordination mechanism (see Sect. 4.3) to modulate the swing phase duration and is set to zero when this mechanism is inactive. Parameters $\hat{\phi}_{AEP}$, $\hat{\phi}_{PEP}$ and $\hat{\omega}$ are defined as functions of the nominal swing phase duration $\hat{T}_{sw}$ and the nominal duty ratio $\hat{\beta}$ ((11) and (12)).

4.2.2 Foot trajectory generation and joint PD control

For each locomotion phase, the foot trajectory is computed between the initial measured position ($\boldsymbol{r}_{LO}$ or $\boldsymbol{r}_{TD}$) and the nominal final position ($\hat{\boldsymbol{r}}_{AEP}$ or $\hat{\boldsymbol{r}}_{PEP}$), in a way that guarantees the continuity of the speed at the transitions. The details of the trajectory generation can be found in Maufroy (2009a) (or on our website, see the link given in the abstract). The velocity profiles of the x and y components of the trajectory are computed and parameterized using the phase ϕ and the nominal foot position is obtained by temporally integrating them.

For the trajectory during the *swing phase*, the nominal speed at AEP is set to $\mathbf{0}$ in order to allow for a smooth landing. Moreover, the trajectory must insure a sufficient toes clearance. The motion is generated using a cycloid trajectory modified to insure speed continuity at liftoff and to be able to specify an offset of the AEP vertical coordinate if needed. This offset $\hat{\Delta}$ (see (9)) has the role to delay the stance phase onset of a foreleg compared to the ipsilateral hind leg (see Sect. 5.1.3).

As the transition to the *stance phase* occurs just after the contact of the foot with the ground, the initial speed for this phase is set to be $\mathbf{0}$. The velocity profile of the x component $v_{st,x}$ is set constant during the stance phase (but for an initial constant acceleration period). For $v_{st,y}$, various profiles have been tested and lead to similar results as long as the velocity is large at the beginning of the stance phase and decreases fast enough afterward. As shown by (10), the horizontal speed at PEP is different from zero. Hence even if ϕ reaches 2π, the backwards motion of the foot continues (as the trajectory is generated by integrating the velocity profiles), allowing for the step length to be bigger than the nominal value $\hat{L}$ if needed.

Based on the nominal position and nominal speed, the reference joint angles and angular velocities ($\tilde{\theta}^i_j$ and $\dot{\tilde{\theta}}^i_j$, with subscript j being the joint index) are computed using the inverse kinematics model of the leg. As the leg is made tri-segmented, we constrained the knee and ankle joint angles to be equal. The joint torques Γ^i_j are then generated using the following PD control law:

$$\Gamma^i_j = K^i_{Pj,p}(\tilde{\theta}^i_j - \bar{\theta}^i_j) + K^i_{Dj,p}(\dot{\tilde{\theta}}^i_j - \dot{\bar{\theta}}^i_j) \tag{14}$$

with:

$$K^i_{Pj,p} = \begin{cases} \hat{c}^i\ \hat{K}_{Pj,p} & \text{for } j \in \{2,3\},\ p = st \\ \hat{K}_{Pj,p} & \text{otherwise} \end{cases} \tag{15}$$

$$K^i_{Dj,p} = \begin{cases} \sqrt{\hat{c}^i}\ \hat{K}_{Dj,p} & \text{for } j \in \{2,3\},\ p = st \\ \hat{K}_{Dj,p} & \text{otherwise} \end{cases} \tag{16}$$

where $\hat{c}^i$ is a parameter used to modulate the PD control gains of the knee and ankle joints during the stance phase.

4.2.3 Transition conditions

The transitions between the swing and stance phases in each LC are regulated using conditions based on the normal ground reaction force f_n (measured by the foot force sensor) which is used as leg loading information. The transition from swing to stance is triggered when the contact of the foot with the ground is detected, or equivalently when the leg loading becomes bigger than 0 (3). On the other hand, the transition from stance to swing is prevented as long as the leg loading is over a certain threshold (5). The nominal force threshold $\hat{\chi}$ is set to a value slightly inferior to one quarter of the model weight. The parameter χ_{mod} is used by the ascending coordination mechanism (see Sect. 4.3) to modulate the force threshold and is set to zero when this mechanism is inactive.

Conditions based on ϕ ((4) and (6)) are added just to prevent undesired early transitions, just after the transfer from one phase to the other, by leaving the time to f_n to sufficiently increase (resp. decrease) just after the touchdown (resp. the liftoff).

4.3 Ascending Coordination Mechanism (ACM)

In the simulation (Fig. 13) shown in Sect. 5.2.2, it is found that the control system is particularly sensible to lateral perturbation decreasing the rolling motion amplitude when we employ no explicit interleg coordination among LCs. Hence, we implemented a two-fold ascending coordination mechanism that brings a solution to the main cause of failure (i.e. the foreleg cannot swing) while limiting the impact on the stability:

1. The stance-to-swing transition in a hind leg (*sH* where *s* stands for either R or L) promotes the same event in the ipsilateral foreleg (*sF*). The force threshold of the foreleg χ^{sF} is linearly increased as ϕ^{sH} increases during the swing phase of the hind leg, as follows:

$$\chi^{sF} = \begin{cases} \hat{\chi} & \text{if } \phi^{sH} < \hat{\phi}_{acm} \\ \hat{\chi} + \chi_{mod} & \text{if } \phi^{sH} \in [\hat{\phi}_{acm}; \hat{\phi}_{AEP}] \\ \hat{\chi} & \text{if } \phi^{sH} > \hat{\phi}_{AEP} \end{cases} \quad (17)$$

$$\chi_{mod} = \frac{\phi^{sH} - \hat{\phi}_{acm}}{\hat{\phi}_{AEP} - \hat{\phi}_{acm}} \cdot \hat{\chi}_{ampl} \quad (18)$$

where $\hat{\phi}_{acm}$ is the modulation threshold and $\hat{\chi}_{ampl}$ is the maximum value of the modulation. $\hat{\phi}_{acm}$ is set to 0.55 $\hat{\phi}_{AEP}$, which is slightly bigger than the value of the hind leg phase ϕ^{sH} at which the stance-to-swing transition occurs in the foreleg in normal conditions. Hence, this part of the mechanism detects the disruption of the normal leg loading and unloading cycle (that prevents the foreleg to swing) and restarts the body rolling motion by forcing the transition to the swing phase in the foreleg. The value of the parameters are given in Table 7 in Appendix.

2. The duration of the next swing phase of the foreleg is shortened, by setting ω_{mod} of (2):

$$\omega^{sF}_{mod} = \frac{f^{sF}_{n,LO} - \hat{\chi}}{\hat{\chi}_{ampl}} \cdot \hat{\omega} \quad (19)$$

where $f^{sF}_{n,LO}$ is the normal ground reaction force measured by the foreleg force sensor at the stance-to-swing phase transition. If greater than $\hat{\chi}$, it indicates that the transition was triggered by the first part of the mechanism so that θ_{roll} is closer from 0 than in the normal conditions (as the rolling motion amplitude is reduced). Hence, this part of the mechanism shortens the swing phase duration to avoid excessive increase of the roll angle in the direction of the swinging foreleg (the value of the roll angle at liftoff is estimated by the load supported by the foreleg at the transition).

5 Simulation results

5.1 Interleg coordination and simulation of walk gait

A gait is a locomotion pattern characterized by phase differences ($\gamma \in [0, 1]$) between the legs during their pitching motion. For low- to medium-speed walking (with $Fr \leq 0.6$ approximately), medium sized cursorial mammals (like cats and dogs) mainly use the walk gait (Orlovsky et al. 1999),[9] while they switch to the trot gait, then the gallop gait at higher locomotion speed (Hildebrand 1968). Hence this section will consider the realization of the walk gait in that range of *Fr* values. Using γ^{cntr} and γ^{ipsi} to refer respectively to the phase differences between contralateral and ipsilateral legs, this gait is characterized by: $\gamma^{cntr} = 0.50$ and $\gamma^{ipsi} \simeq 0.25$. Sections 5.1.1 to 5.1.3 presents the ideas and concepts underlying the control strategy, while Sect. 5.1.4 gives an overview of the experiments that were carried out regarding the issue of interleg coordination.

5.1.1 Leg loading transfer mechanisms

There are mainly two mechanisms acting during the locomotion to transfer the load induced by the weight of the body between the supporting legs:

- The *longitudinal transfer* of leg loading is related to the forward motion of the body (i.e. the translation along its roll axis) with respect to the positions of the feet of the supporting legs. This mechanism results in a progressive transfer of leg loading from the supporting legs in a backward position to the ones in a forward position.
- The *lateral transfer* of leg loading is related to the lateral motion of the body (i.e. the translation along its pitch axis) with respect to the positions of the feet of the supporting legs. With our simple mechanical model, this latter is closely related to the rolling motion.

Contrary to the longitudinal transfer which is present even when the motion is restricted to the sagittal plane, lateral transfer of leg loading only appears when the interaction between the stepping motions of the legs and the rolling motion is involved, i.e. when the locomotion is considered in three dimensions.

5.1.2 Emergence of contralateral alternate stepping

Even with the simplest control system configuration, i.e four leg controllers operating *independently*, stable coordinate walking patterns emerge in a broad range of parameter values. All the patterns are characterized by an *contralateral alternate stepping* coordination, in which contralateral legs are stepping alternatively, i.e. $\gamma^{cntr} = 0.50$. The mechanism underlying the emergence of such coordination is schematically explained in Fig. 4, when considering the motion in the frontal plane.

If we consider that both legs on one side (the right side for example) are in the swing phase,[10] the system, equivalent to an inverted pendulum, starts to rotate around the axis joining

[9] Alexander (1992) also mentioned that cats change the gait from a walk to a trot at 1.0 m/s ($Fr = 0.7$) approx.

[10] The realization of this situation can be insured at the beginning of the simulation by explicitly triggering the transition to the swing phase.

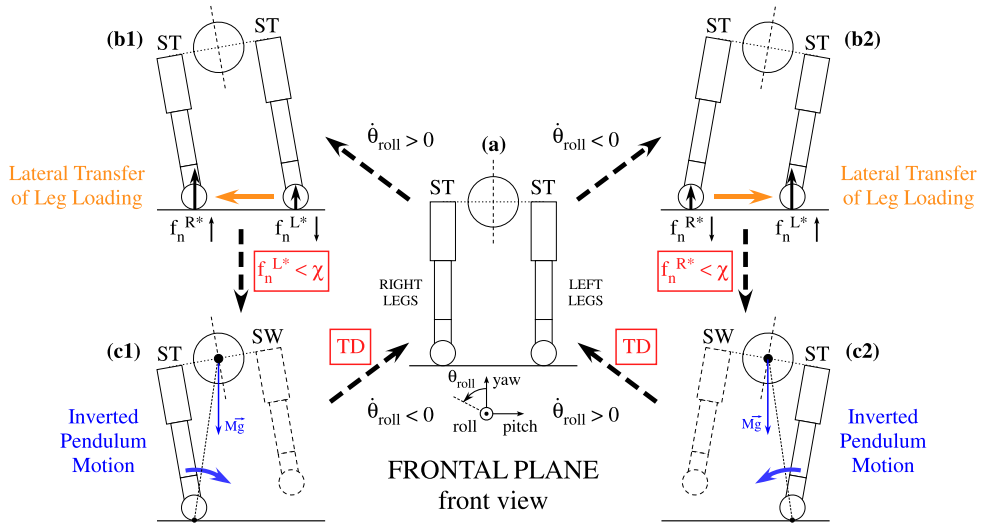

Fig. 4 Contribution of the phase modulations to the emergence of alternate stepping coordination. When both right legs are in the swing phase, rolling motion is generated as the system is equivalent to an inverted pendulum (**c2**). As rolling and lateral motions of the body are directly related, the body also starts to move laterally. After the touchdown of the swinging legs (**a**), the load is transferred laterally from the left to the right legs (**b1**). This unloads the left legs and the transition to swing is triggered when f_n becomes smaller that the threshold χ (**c1**). The same sequence of events is repeated in the other direction (succession of (**a**), (**b2**) and (**c2**)) and then periodically

the contact points of the left feet with the ground (as represented in Fig. 4(c2)). Due to the moment induced by gravity, rolling motion is generated ($\dot{\theta}_{roll} > 0$), which also induces the lateral motion of the body. After the touchdown[11] of the swinging legs (a), rolling and lateral body motions cause the lateral transfer of the load from the left to the right legs (b1). This progressively unloads the left legs that were formerly supporting the body and the transition to swing is triggered when f_n becomes smaller that the threshold χ (c1). The same sequence of events is repeated on the other side as $\dot{\theta}_{roll}$ becomes negative (succession of (a), (b2) and (c2)) and then periodically. Hence, although the phase modulations in the LCs are carried out in a distributed fashion, as they are grounded on leg loading information which is influenced by the global state of the system (via the lateral transfer of leg loading for example), they result in the mutual entrainment of the stepping motions of the legs (in the sagittal plane) and the body rolling motion (in the frontal plane). As a consequence, contralateral alternate stepping emerges, even though there is no interleg coordination mechanism linking the contralateral legs.

5.1.3 Adjustment of the ipsilateral phase difference

With identical parameters for the fore- and hind leg LCs, the walk gait could not be realized and the walking patterns that were generated in those cases were all pace gaits.[12] This indicated that an additional mechanism was needed to delay the stepping of the foreleg relative to its ipsilateral hind leg stepping in order to realize a walk gait. This was achieved using the idea that the timing of the stance phase onsets in the fore- and hind legs can be manipulated by adjusting the nominal AEP vertical coordinate via the offset $\hat{\Delta}$ (9), as illustrated in Fig. 5. As the body is animated with a rolling motion during the common swing phase of ipsilateral legs, increasing (resp. decreasing) $\hat{\Delta}$ of one LC result in the delay (resp. the advance) of the touchdown the corresponding leg. Accordingly, while setting $\hat{\Delta}^{*H}$ to 0, increasing $\hat{\Delta}^{*F}$ progressively increases the value of γ^{ipsi}, until the point where phase differences characteristic of a walk gait is generated (see Fig. 8(a)). One example of such walk gait is represented in Fig. 6.

This coordination mechanism fulfills the same function as an ascending inhibitory coupling, that would explicitly insure a phase difference between the ipsilateral legs. With our approach, the phase delay is induced by taking advantage of the embodiment (here the rolling motion), while keeping the LCs independent.

[11] The touchdown of both legs is represented as being simultaneous for the sake of simplicity. This is however not generally the case as, for the walk gait for example, the touchdown of the hind leg precedes the one of the foreleg.

[12] To distinguish between walk and pace gaits, we use the intermediate value of 0.125 as a limit. Hence, if γ^{ipsi} is larger than 0.125, we consider that the gait is a walk, while, if it is smaller, we classify it as a pace.

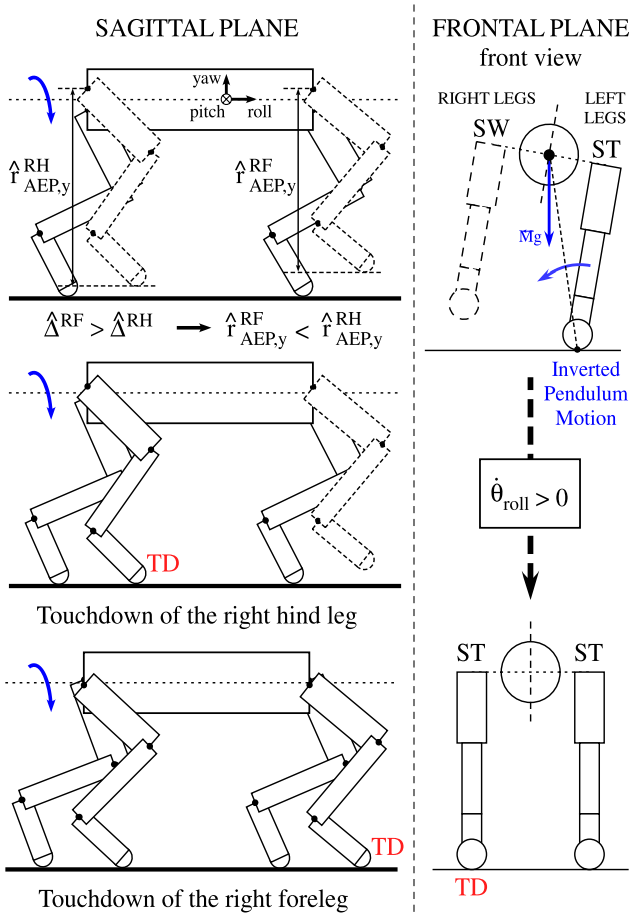

Fig. 5 Illustration of the influence of the nominal AEP vertical coordinate offset $\hat{\Delta}$ on γ^{ipsi}. For $\hat{\Delta}^{*F} > \hat{\Delta}^{*H}$, as the body rotates around the roll axis, the touchdown of the hind leg occurs earlier than the one of the foreleg, hence resulting in the increase of the ipsilateral phase difference γ^{ipsi}

5.1.4 Modulation of the walking patterns

Methods At the beginning of the simulation, the model starts with the four legs touching the ground, in a vertical position (the foot position is the vertical projection of the hip position on the ground). Locomotion is initiated by setting the phase of the right leg controllers to the swing, which induce the first stepping and start the body rolling oscillation. Parameters are set to generate first a walking pattern with a short cyclic period (typically $\bar{T} \simeq 0.4$ s), which has a small rolling motion amplitude, as it is the easiest when starting from a situation with no rolling motion. After convergence of the walking pattern characteristics (which takes a few seconds), the parameter(s) under investigation is (are) continuously varied to their modified values.

Influence of the phase dynamics parameters Modulation of the walking speed and the cyclic period $\bar{T}$ of the walking patterns (shown in Fig. 10) is achieved by modifying parameters at the phase dynamics level: the nominal swing phase duration $\hat{T}_{sw}$ and the nominal duty ratio $\hat{\beta}$. These two parameters directly influence the speed of the backward motion of the leg during the stance (10), so that the decrease of the nominal duty ratio and/or the nominal swing phase duration results in a decrease of the walking speed. On the other hand, as its nominal value is given by $\hat{T} = \hat{T}_{sw}/(1-\hat{\beta})$, the cyclic period increases when the nominal duty ratio and/or the nominal swing phase duration increase. The influence on the cyclic period however is indirect, because the phase transitions are controlled using sensory information ((3) and (4)).

The modulations of the walking speed and the cyclic period $\bar{T}$ are accompanied with the adaptations of the step parameters, including $\bar{\beta}$, $\bar{L}$, Θ and so on (Maufroy 2009a). In particular, adaptations of the gait (via the adaptation of γ^{ipsi}) also occur. Although the detail of these gait adaptations is rather complex, their general tendencies reflect changes in the relative importance of the two leg loading transfer mechanisms presented in Sect. 5.1.1:

- increased influence of the *lateral transfer* of leg loading (due to large rolling motion amplitude for example), results in the simultaneous loading/unloading of the ipsilateral legs, hence promoting in-phase stepping of these legs, i.e. a decrease of γ^{ipsi}.
- increased influence of the *longitudinal transfer* of leg loading (due to the large forward motion of the body during the stance phase) results in the delayed unloading of a foreleg compared to its ipsilateral hind leg, hence promoting the increase of γ^{ipsi}.

Hence, increasing the nominal swing phase duration $\hat{T}_{sw}$ (while keeping the nominal duty ration $\hat{\beta}$ constant) causes the increase of the cyclic period and the decrease of the speed. As the period increases, the rolling motion amplitude becomes larger, being proportional to the square of the period (Kimura et al. 1990), which increases the influence of the lateral transfer of leg loading. As a result, the ipsilateral phase difference γ^{ipsi} decreases ant the gait progressively shifts to a pace. For example, the ipsilateral phase difference γ^{ipsi} varies from $\sim$0.21 (indicating a walk gait), to $\sim$0.15 and finally $\sim$0.05 (which is characteristic of a pace) when $\hat{T}_{sw}$ is successively set to 0.15 s, 0.20 s and finally 0.25 s (with the other parameters set as follows: $[\hat{\beta}, \hat{c}^{*H}, \hat{c}^{*F}] = [0.75, 2, 1.7]$ and $[\hat{\Delta}^{*H}, \hat{\Delta}^{*F}] = [0, 0.01]$ (m)).

On the other hand, decreasing the nominal duty ratio $\hat{\beta}$ (while keeping the nominal swing duration $\hat{T}_{sw}$ constant) causes the speed to increase while the cyclic period decreases. The adaptations of the main step parameters with the speed as $\hat{\beta}$ is decreased from 0.75 to 0.50 (by steps of 0.05), with $\hat{T}_{sw} = 0.15$ s is shown in Fig. 7. As the stance phase termination is regulated by the leg unloading condition (5), $\hat{\beta}$ has no direct influence on the stance phase duration. Hence, the increase of the speed is mainly due to the lengthening of the stride (a) (which is multiplied by a factor

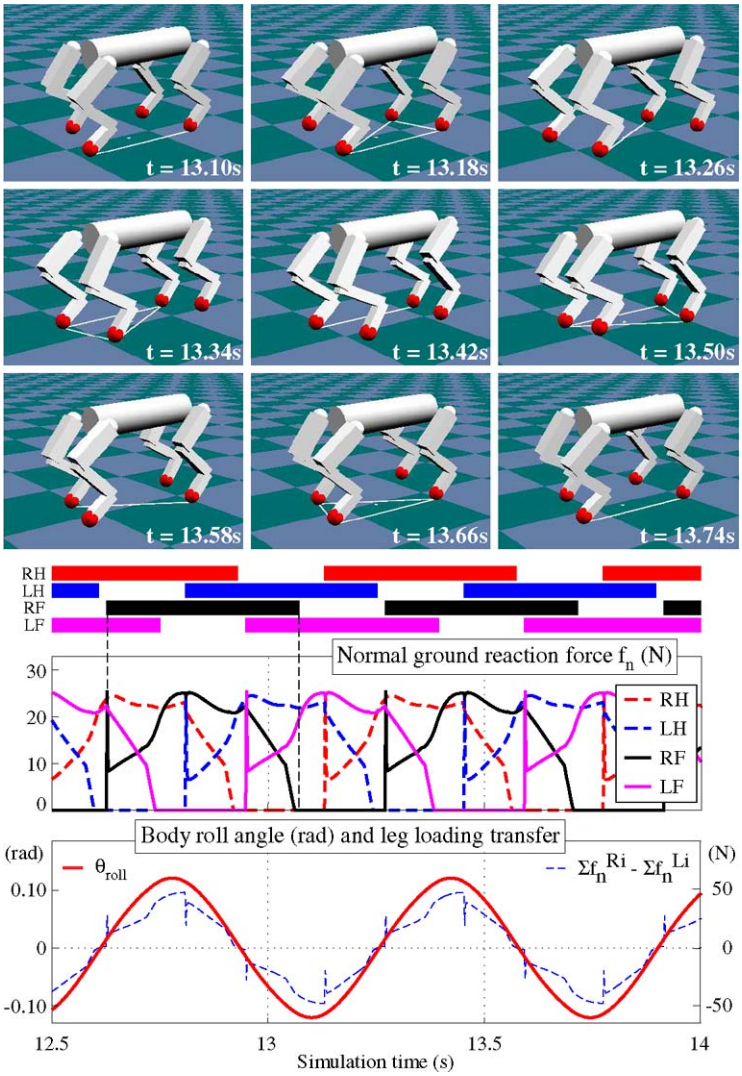

Parameter settings					
$\hat{T}_{sw}$	(s)	0.25	$\hat{\beta}$		0.75
$\hat{\Delta}^{*F}$	(m)	0.02	$\hat{\Delta}^{*H}$	(m)	0.00
$\hat{c}^{*F}$		1.00	$\hat{c}^{*H}$		1.00

Fig. 6 By taking advantage of the emergent alternate coordination and adjusting the phase difference γ^{ipsi} using the nominal AEP vertical coordinate offsets $\hat{\Delta}$, walk gait was realized with independent leg controllers. This figure represents a walking pattern characterized by a cyclic period $\bar{T} \simeq 0.65$ s, a duty ratio $\bar{\beta} \simeq 0.69$ and an ipsilateral phase difference $\gamma^{ipsi} \simeq 0.22$. These values are quite different from the values that would be expected when considering the nominal parameters (given in the lower table): $\hat{\beta} = 0.75$ and $\hat{T}_{sw} = 0.25$ s, resulting in $\hat{T} = 1.0$ s. This shows that the motion is strongly influenced by the phase modulations. The difference between the load supported by the right and the left legs is represented together with the rolling motion, showing that the lateral transfer of leg loading occurs in phase with this latter

of ∼2.4), rather than the shortening of the cyclic period (b) (which is divided by a factor of only ∼1.3). As the travel of the body during the stance phase increases, the increasing influence of the longitudinal transfer of leg loading contributes to shift the load supported by ipsilateral legs from the hind to the front. Stance-to-swing transition then occurs earlier (resp. later) for the hind leg (resp. foreleg), causing the increase of γ^{ipsi} (c), so that the gait becomes closer to a trot. As the period during which both ipsilateral legs are in the swing phase is then reduced, the rolling motion amplitude decreases (d), while the cyclic period, which is related to this latter (Kimura et al. 1990) shortens (b). As $\hat{T}_{sw}$ is con-

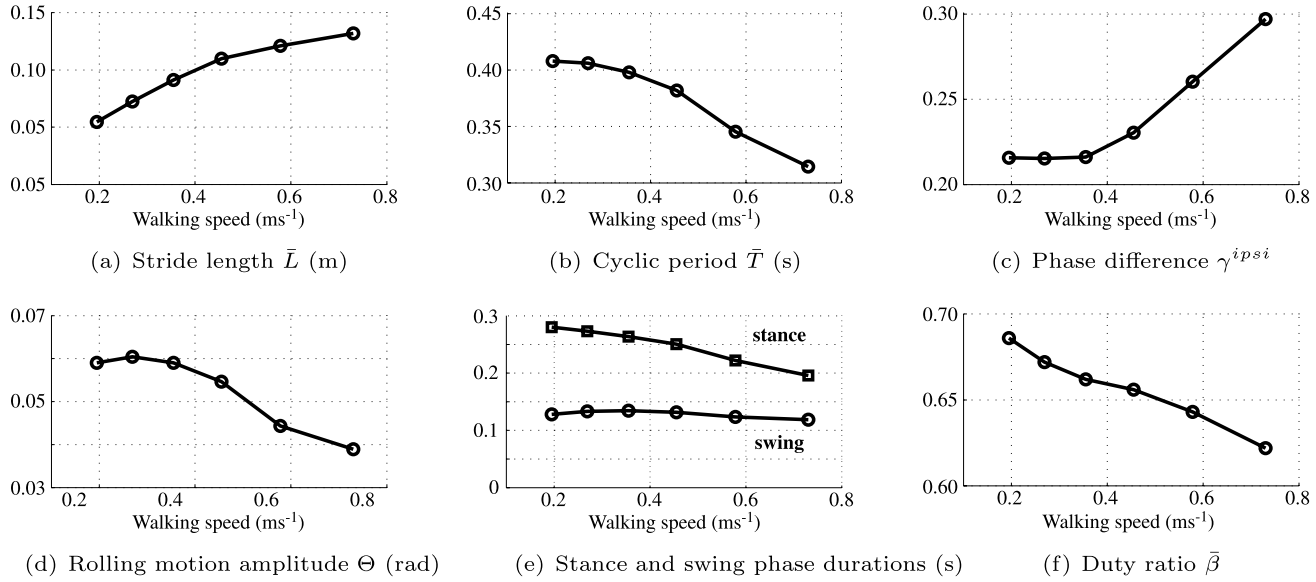

(a) Stride length $\bar{L}$ (m) (b) Cyclic period $\bar{T}$ (s) (c) Phase difference γ^{ipsi}

(d) Rolling motion amplitude Θ (rad) (e) Stance and swing phase durations (s) (f) Duty ratio $\bar{\beta}$

Fig. 7 Adaptations of the main step parameters with the speed (as $\hat{\beta}$ is decreased from 0.75 to 0.50 by steps of 0.05, with $\hat{T}_{sw} = 0.15$ s). The values of the AEP offsets and PD gain coefficients are set as follow: $[\hat{\Delta}^{*H}, \hat{\Delta}^{*F}] = [0, 0.01]$ (m) and $[\hat{c}^{*H}, \hat{c}^{*F}] = [2, 1.7]$

stant, the swing phase duration is mostly fixed (variation of ∼10%), while it is the stance phase duration which varies (decrease of ∼30%) (e). Hence, a reduction of the effective duty ratios $\bar{\beta}$ is also observed (f).

The gait variations that occur together with modifications of $\hat{T}_{sw}$ and $\hat{\beta}$ are undesirable, first, regarding our objective (which is to realize a walk gait), but also from the point of view of the stability and the resistance ability to perturbations. Indeed, pace gaits are associated with large rolling motion amplitude (likely because the swing phases of ipsilateral legs largely overlap), which results in walking patterns much less resistant to perturbations than walk gaits. Inversely, when the gait is changing in the direction of a trot, we observed that the locomotion becomes instable when γ^{ipsi} becomes too large. This is likely due to the observed decrease of rolling motion amplitude which accompanies the increase of γ^{ipsi} (Fig. 7(d)). As a result, lateral transfer of leg loading is decreased and when it becomes too low, the contralateral alternate stepping coordination provided by the phase modulations (Sect. 5.1.2) is impaired and leg coordination is lost, resulting in the fall of the model.

Influence of the trajectory generation parameters The variations of the ipsilateral phase difference γ^{ipsi} related to modifications of $\hat{T}_{sw}$ and $\hat{\beta}$ can be attenuated by the adjustments of the following two parameters, defined at the trajectory generation level:

- the nominal AEP vertical coordinate of the forelegs, using the nominal offset $\hat{\Delta}^{*F}$ (9). As explained in Sect. 5.1.3, increasing $\hat{\Delta}^{*F}$ allows to increase γ^{ipsi}, as represented in Fig. 8(a);
- the mechanical impedance of the legs during the stance phase, using coefficients $\hat{c}^i$ to adjust the PD control gains (14). Increasing the PD control gains of both the fore and hind legs were found to result in the decrease of γ^{ipsi} (as shown in Fig. 8(c)).

Adjustment of the parameters to realize a walk gait The influence on the gait of the four parameters presented above are summarized in Table 3. To maintain the walk gait (i.e. keep γ^{ipsi} within [0.20, 0.30] approximatively), the increase of the nominal swing phase duration $\hat{T}_{sw}$ is combined with the increase of $\hat{\Delta}^{*F}$ and the decrease of the PD gains coefficients $\hat{c}^i$, while inverse adjustments are used when decreasing the duty ratio. These adjustments are represented in Fig. 9, which shows that larger adjustments are required when varying the nominal swing phase duration than the nominal duty ratio.

As a result, a walk gait could be realized in a broad range of speeds and cyclic periods, corresponding to $Fr \in [0.05, 0.55]$ approximatively (see Fig. 10). Such low speed dynamic walking with long cyclic period was not realized in our former studies (Fukuoka et al. 2003; Kimura et al. 2007; Kimura and Fukuoka 2004). Moreover, the walking patterns are generated with independent leg controllers.

5.2 Stabilization of the posture and resistance ability against perturbations

In this section, the mechanism of posture stabilization provided by the phase modulations is first explained. The resistance ability against perturbations of the control system without ACM (independent LCs) and with it is evaluated

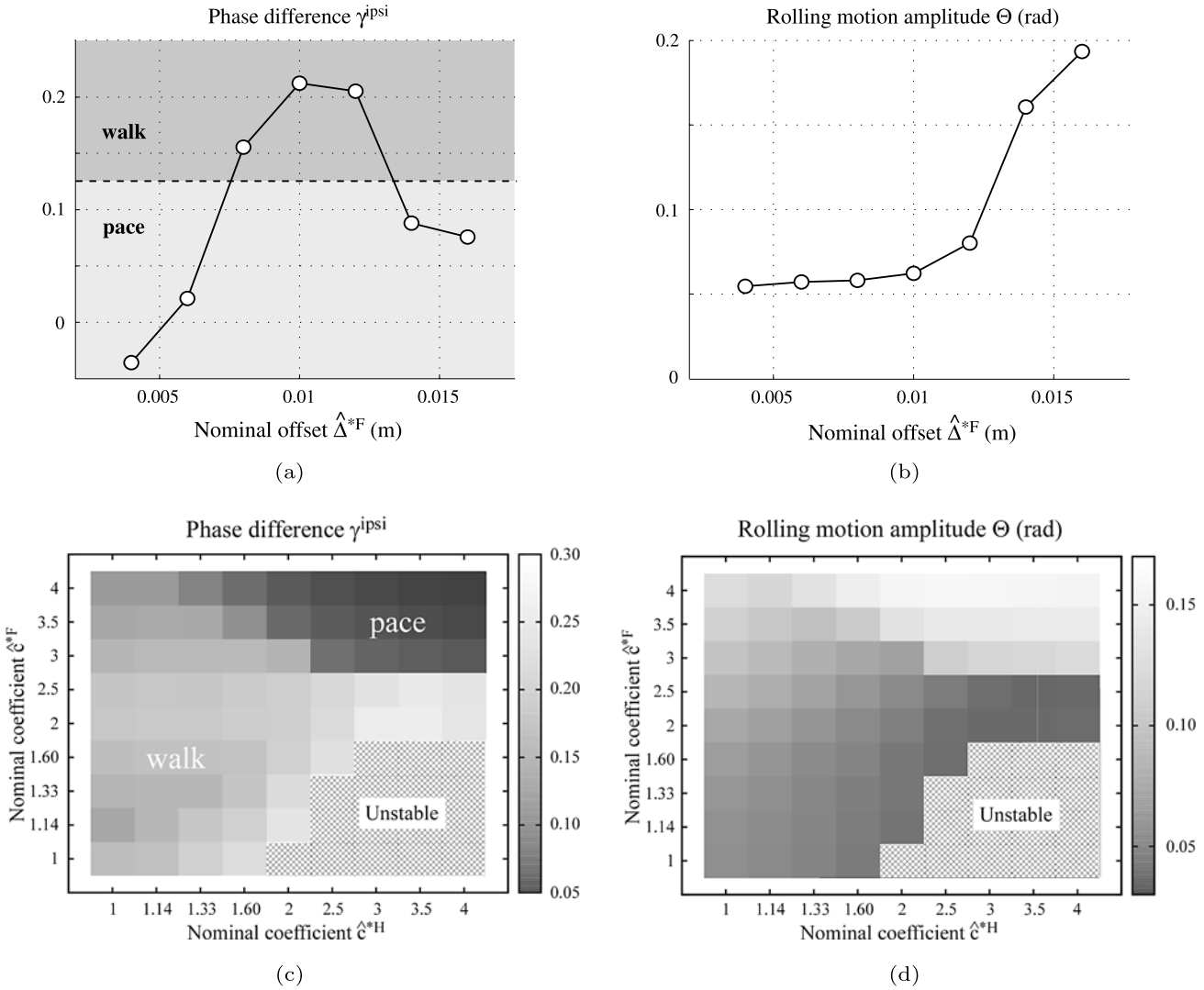

Fig. 8 Illustration of the influence on the gait of the trajectory generation parameters: the foreleg AEP offset $\hat{\Delta}^{*F}$ (*upper graphs*) and the PD gains coefficients $\hat{c}^i$ (*lower graphs*). All the experiments were carried out with $[\hat{T}_{sw}, \hat{\beta}] = [0.15\text{ s}, 0.75]$. In the *upper graphs* (**a**) and (**b**), the values of the PD gains coefficients and the hind legs AEP offset are fixed (resp. $\hat{c}^{*H} = \hat{c}^{*F} = 2$ and $\hat{\Delta}^{*H} = 0$), while the value of the foreleg AEP offset varies. As explained in Sect. 5.1.3, increasing $\hat{\Delta}^{*F}$ allows to increase of the ipsilateral phase difference, resulting in the switching of the gait from pace to walk (**a**). This strategy however has its limitation, as further increase of $\hat{\Delta}^{*F}$ results in a larger rolling motion amplitude, which causes γ^{ipsi} to drop because of the increased influence of the lateral transfer of leg loading. The *lower graphs* (**c**) and (**d**) show the results of experimentations which investigate the influence of the PD gains coefficients $\hat{c}^i$. In that case, the AEP offsets are set as follows: $[\hat{\Delta}^{*H}, \hat{\Delta}^{*F}] = [0, 0.01]$ (m). As shown in (**c**), at high values of $\hat{c}^{*H}$ and $\hat{c}^{*F}$, the gait switches to a pace, as the ipsilateral phase difference decreases. This is accompanied with the increase of the rolling motion amplitude, as shown in (**d**)

Table 3 Summary of the influence of the leg controller parameters on the gait (characterized by the ipsilateral phase difference γ^{ipsi})

Increase of:	$\hat{T}_{sw}$	$\hat{\beta}$	$\hat{\Delta}^{*F}$	$\hat{c}^i$
Influence on γ^{ipsi}	Decrease	Decrease	Increase	Decrease

via various perturbations of the walking patterns (lateral perturbations and terrain irregularities). The simulations were carried out using two walking patterns with different cyclic periods (Table 4).

5.2.1 *Posture stabilization in the frontal plane*

The stabilization mechanism provided by the phase modulations based on leg loading/unloading is schematically represented in Fig. 11. Considering first the case where a perturbation directed to the left is applied, the rolling motion of the body becomes asymmetric so that the model is leaning toward the left side during the walking. In other words, the average body rolling angle over the cyclic period when the perturbation is applied becomes negative, i.e. $\langle \theta_{roll} \rangle_k < 0$ (using the definition given in Table 2). The asymmetry of

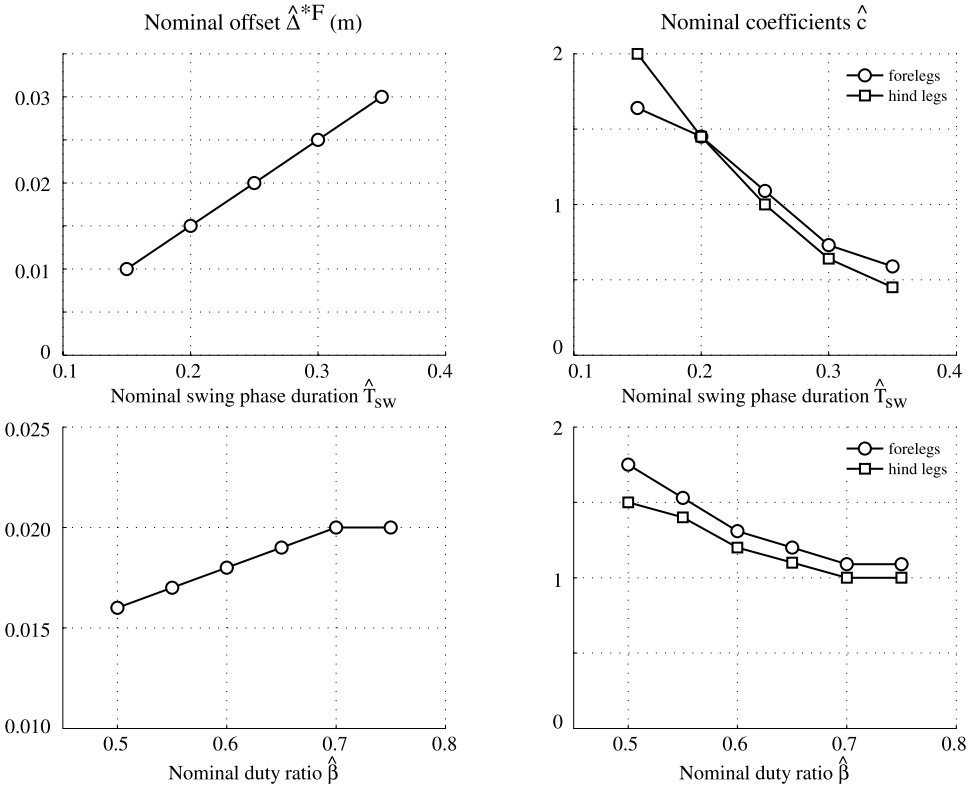

Fig. 9 When $\hat{T}_{sw}$ is *increased* (here from 0.15 to 0.35 s, with $\hat{\beta} = 0.75$), offset $\hat{\Delta}^{*F}$ and coefficients $\hat{c}$ must respectively be increased (*left upper graph*) and decreased (*right upper graph*). Inverse adjustments (*left* and *right lower graphs*) are required when $\hat{\beta}$ is *decreased* (here from 0.75 to 0.50, with $\hat{T}_{sw} = 0.25$ s)

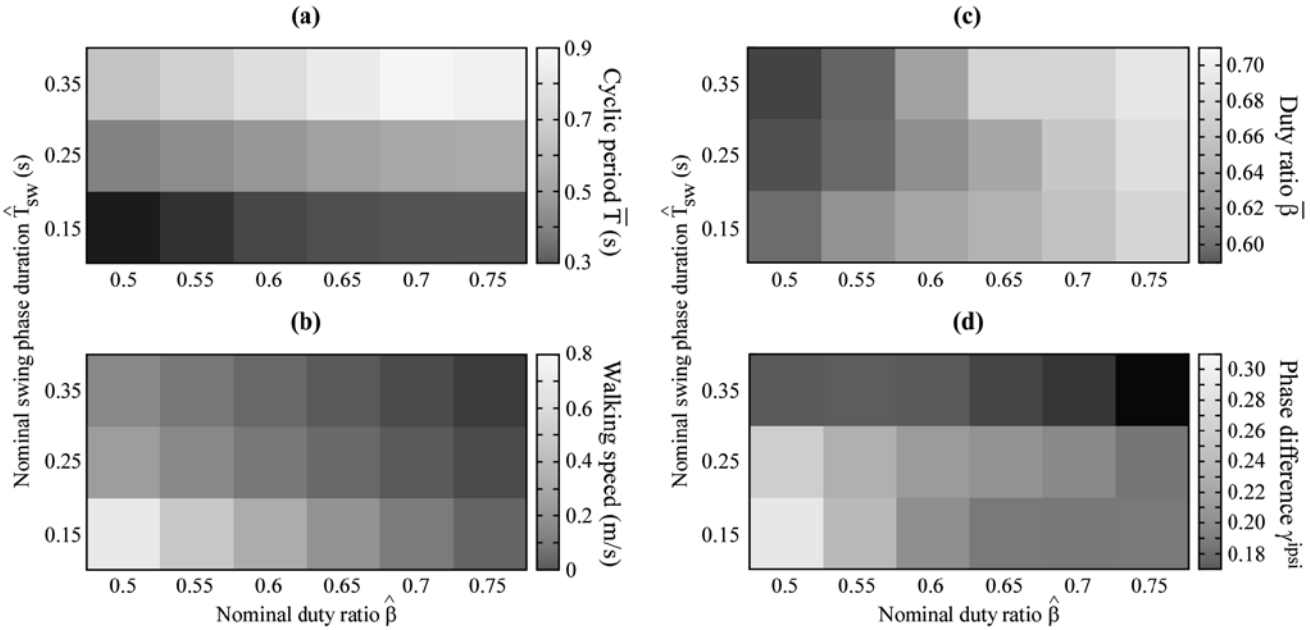

Fig. 10 With the adjustments represented in Fig. 9, walk gait (with γ^{ipsi} within [0.20, 0.30] approximatively) was realized in a broad range of *Fr* values ($Fr \in [0.05, 0.55]$) when varying the nominal swing phase duration $\hat{T}_{sw}$ and duty ratio $\hat{\beta}$. This figure represents the main characteristics of the walking patterns, i.e. the cyclic period (**a**), the walking speed (**b**), the duty ratio (**c**) and the ipsilateral phase difference (**d**). For the modulations of the speed, the results follow closely the tendencies given by (10). Regarding the modulation of the cyclic period $\bar{T}$, results for the variation of the nominal swing phase duration are consistent with what could be expected from the variation of its nominal value $\hat{T}$ (for example the increase of $\hat{T}_{sw}$ by a factor of 2.3, from 0.15 to 0.35 s, results in the increase of $\bar{T}$ by a factor of ∼2.2). In contrast, the variation of the cyclic period when the nominal duty ratio varies is much smaller than expected (decrease by a factor of ∼1.25 instead of 2 when $\hat{\beta}$ varies from 0.75 to 0.50)

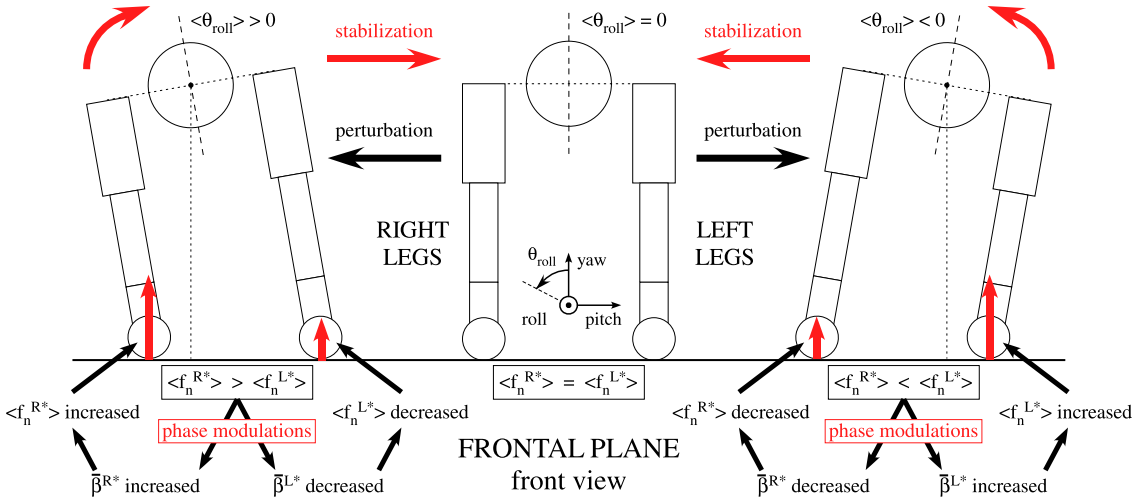

Fig. 11 Stabilization mechanism provided by the phase modulations, relying on automatic adjustments of the duty ratios (index k was omitted to simplify the figure). When the body rolling motion becomes asymmetric (i.e. $\langle\theta_{roll}\rangle \neq 0$) due to a perturbation, the average load $\langle f_n\rangle$ supported by the left and right legs differs. This results in the increase (resp. the decrease) of the stance phase duration as the leg is more (resp. less) loaded, due to the phase modulations. Hence the effective duty ratios $\bar{\beta}$ are automatically adjusted and the original difference between $\langle f_n\rangle$ in the right and left legs is amplified to generate a stabilizing moment that tends to cancel the asymmetry

the rolling motion causes a similar asymmetry in the load supported by the legs so that $\langle f_n^{L*}\rangle_k$ becomes greater than $\langle f_n^{R*}\rangle_k$. As f_n is used to modulate the transition from the stance to the swing phase, the increase of $\langle f_n\rangle_k$ (for the left legs) leads to the prolongation of the stance phase, while it is shortened when $\langle f_n\rangle_k$ decreases (for the right legs). Consequently, the effective duty ratios of the left legs increase, while they decrease for the right legs ($\bar{\beta}_k^{L*} > \bar{\beta}_k^{R*}$), amplifying the original asymmetry of the $\langle f_n\rangle_k$. This is equivalent to say that the duration of the inverted pendulum motion around the left legs feet (situation (c2) in Fig. 4) becomes longer than the one around the right legs feet (situation (c1)) during walking cycle k. Hence, via the automatic adjustment of the duty ratios, a moment is generated that tends to cancel the asymmetry of the rolling motion and bring $\langle\theta_{roll}\rangle_{k+1}$ back to 0 and therefore contributes to stabilize the posture in the frontal plane. The same argumentation can also be applied, of course, for perturbations that cause an asymmetry of the body rolling motion in the opposite direction.

5.2.2 *Performances against lateral perturbations*

Methods Each simulation in this section started with the same initial conditions as described in the Methods of Sect. 5.1.4. As lateral perturbation, a force, that pushes the model to the left, is applied at the center of mass of the trunk during 0.1 s at various timings during the walking cycle, after the system has reached its steady state. Four timings were chosen: the onset of the swing phase of the left hind leg, left foreleg, right hind leg and right foreleg (respectively indicated by t_{LH}, t_{LF}, t_{RH} and t_{RF}). When the system was able to recover from the perturbation back to the steady state, the trial was considered successful. For each timing, simulations were carried out with increasing intensity of the perturbation force (increased per step of 1 N) until the model was unable to recover and fell.

Table 4 Walking patterns used for the assessment of the resistance ability against perturbations. (SH) and (LG) are walking patterns with respectively a short and a long cyclic period

	$\hat{T}_{sw}$ (s)	$\hat{\beta}$	$\bar{T}$ (s)	$\bar{\beta}$
(SH)	0.15	0.75	0.40	0.69
(LG)	0.25	0.75	0.65	0.69

Table 5 Maximum lateral perturbation force supported by the model without falling according to the timing of application. The ability of the system to recover from perturbations that occur at either t_{RH}, t_{RF} or t_{LF} is relatively good. In those cases, it can withstand perturbation forces whose amplitude are ranging from 10 to 20 N (i.e. 25% to 50% of the weight of the model approximately). However, the model is relatively sensitive to perturbations applied at t_{LH}

	t_{LH}	t_{LF}	t_{RH}	t_{RF}
(SH)	2 N	16 N	14 N	20 N
(LG)	3 N	12 N	10 N	14 N

Independent LCs In the case of independent LCs (the ACM is disabled), results presented in Table 5 shows that the ability to recover from perturbations that occur at either t_{RH}, t_{RF} or t_{LF} is relatively good while, on the other hand, the model is relatively sensitive to perturbations applied at t_{LH}.

For all timings, the perturbation is directed to the left of the model, which causes the angular velocity of rolling $\dot{\theta}_{roll}$ to decrease (Fig. 11). Accordingly, the stance and swing phase duration adjustments due to the phase modulations are qualitatively similar and result in $\bar{\beta}^{L*} > \bar{\beta}^{R*}$. The difference of performance is related to the influence of the perturbation on the amplitude of the body rolling motion and the associated lateral transfer of leg loading. This is illustrated in Figs. 12 and 13 using walking pattern (LG). Graphs showing similar results for (SH) can be found in Maufroy et al. (2009b).

When the perturbation is applied at t_{LF}, t_{RH} or t_{RF}, it results in the *increase* of $|\dot{\theta}_{roll}|$, leading to a temporary augmentation of rolling motion amplitude (see Fig. 12). As a consequence, the lateral transfer of leg loading is accelerated. The additional load supported by the left legs causes their stance phase to be extended, while the swing phase of the right legs is prolonged. For those timings of application of the perturbation, the model fails when the perturbation is so large that the stabilizing moment provided by the duty ratios adjustments is insufficient to cancel the moment induced by the perturbation. The model then falls on the side towards which is directed the perturbation force.

On the other hand, for t_{LH}, the perturbation causes $|\dot{\theta}_{roll}|$ to *decrease*, leading to a temporary diminution of the rolling motion amplitude (see Fig. 13). This tends to cancel the rolling motion and the associated lateral transfer of leg loading. Accordingly, the rate of unloading of the left foreleg decreases and, if the amplitude of the perturbation is large enough, f_n^{LF} does not become smaller than the threshold χ. The transition to the swing phase is prevented, which greatly disturbs the interleg coordination. Depending on the walking pattern, the transition can either only be temporarily prevented (and takes place during the next cycle) such as in Fig. 13 (with (LG) walking pattern) or be durably prevented (when a perturbation of 3 N is applied at t_{LH} with (SH) walking pattern for example, see Maufroy et al. 2009b). In the first case, even if the transition finally occurs, it does with a timing quite different from the usual one. Hence, the model is destabilized and falls on the side. On the other hand, when the transition is durably prevented, none of the forelegs can swing and the model falls forward.

Effectiveness of the ACM The upper considerations show that an additional mechanism is needed to help the system to recover when the rolling motion amplitude is suddenly reduced. The situation that occurs in that case can be seen as a conflict between the control of the rhythmic pitching motions of the legs, which requires the stance-to-swing phase transition of the foreleg to preserve the coordination, and the posture control in the frontal plane, prevents it because a leg still supporting the body should not swing to preserve the balance. For that reason, the ascending coordination mechanism (ACM) described in Sect. 4.3 was introduced at that point. While allowing the foreleg to swing, the ACM globally increases the duty ratio of the foreleg: the transition to the swing phase is still delayed compared to normal (hence the stance phase is extended) while the next swing phase duration is shortened. Moreover, the increase of the duty ratio is positively related with the increase of the load supported by the foreleg (i.e. with the intensity of the perturbation). Consequently, the ACM works in cooperation with the stabilization provided by the phase modulations (Fig. 14). In order to see its effectiveness, we simulated similar perturbation for t_{LH} with ACM (Fig. 14) and we found that adding the ACM to the control system leads to the drastic improvement of the resistance to perturbations applied at t_{LH}, up to 25 N and 16 N for (SH) and (LG) respectively. The ACM did not however improve the performances for the other timings (i.e. t_{LF}, t_{RH} and t_{RF}), where the cause of failure is the excessive increase of the rolling motion.

Importance of the phase modulations based on leg unloading To clarify the contribution of the phase modulations based on leg unloading to the performances, we also investigated the situation where a condition based on the oscillator phase ϕ is used for the control of the stance-to-swing transition, instead of the condition based on leg unloading. In these experiments, after the system has reached its steady state, the condition given by (5) is replaced by: $\phi > \phi_{thres}$, where the threshold ϕ_{thres} is set to the value of ϕ at which the transition normally occurs when the leg-unloading-based condition is used. If the walking pattern maintains after switching the condition, lateral perturbations were applied to evaluate its ability to reject them.

In the case of a short cyclic period (i.e. with walking pattern (SH)), the walk gait is preserved after the switching of the transition conditions. However, very small perturbation forces (∼2 N) caused the loss of interleg coordination resulting in the fall of the model, regardless of the timing (i.e. regardless of the influence of the perturbation on the rolling motion). For walking patterns with longer cyclic period (such as walking pattern (LG)) where the rolling motion amplitude is larger, the locomotion became unstable directly after the condition is changed. Hence, these experiments confirm that the stance termination mechanism based on leg loading/unloading is important for the stabilization of the walking pattern and its resistance to perturbations.

5.2.3 Performances on uneven terrain

Methods Each simulation in this section started with the same initial conditions as described in Sect. 5.1.4. The performances of the control system (with and without the ascending coordination mechanism) when coping with two

Fig. 12 Recovery from a perturbation increasing the amplitude of the rolling motion (a force of 12 N is applied at t_{RF} with walking pattern (LG)). Due to the phase modulations, the duty ratios are automatically adjusted, which contributes to stabilize the posture in the frontal plane and restore the symmetry of the rolling motion

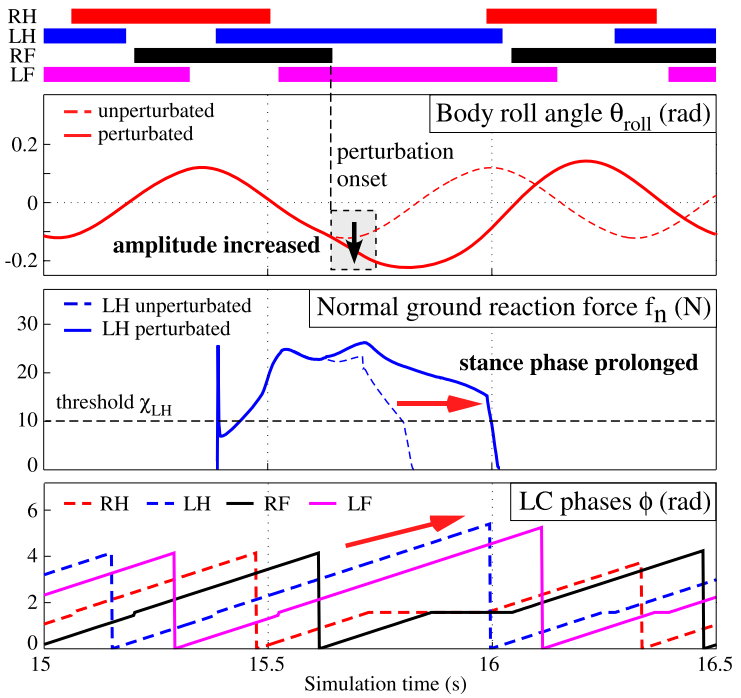

(a) Modulation of the stance period of the supporting legs. The perturbation induces an additional load on the supporting legs (represented by LH here), so that their stance phase is extended. Consequently, the duration of the inverted pendulum motion around the left feet is extended.

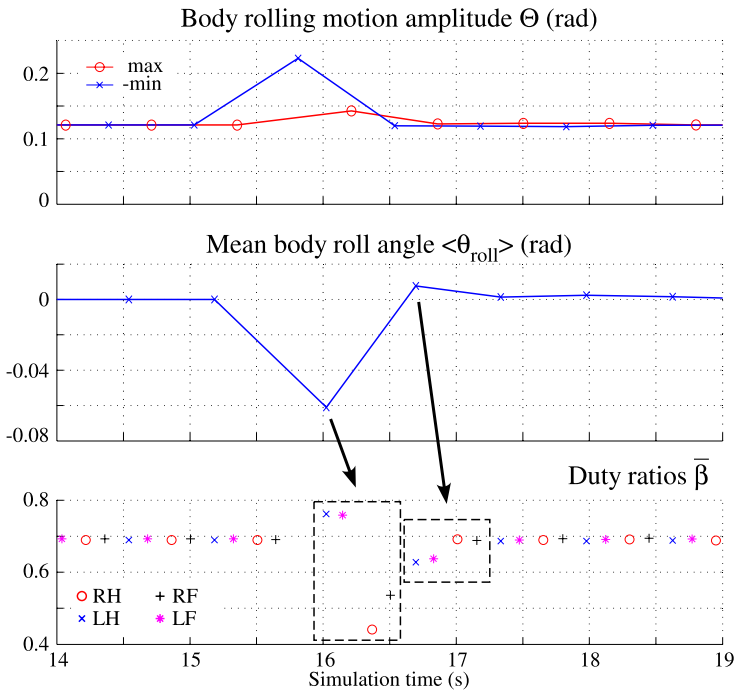

(b) Duty ratios adjustments subsequent to the perturbation. For a mean body roll angle $\langle\theta_{roll}\rangle < 0$ (respectively > 0), the duty ratios of the left legs are increased (respectively decreased) while the ones of the right legs are decreased (respectively increased).

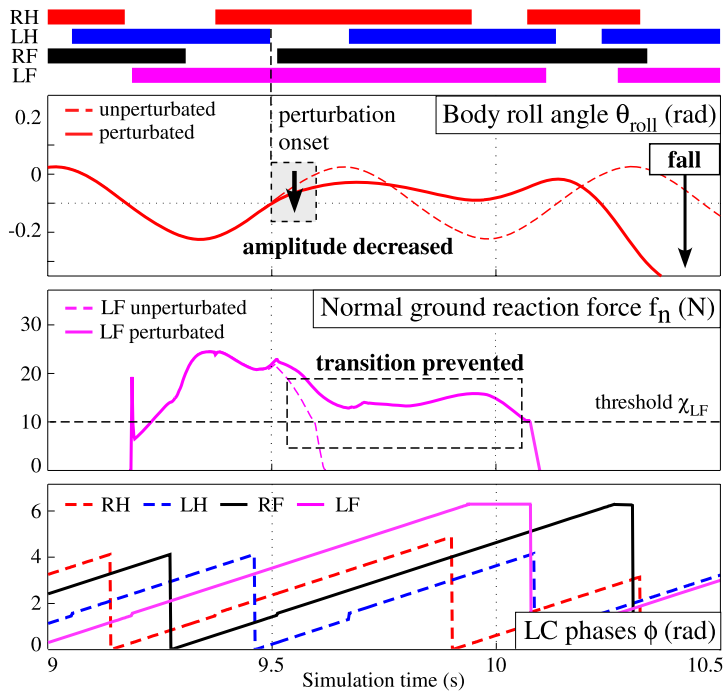

Fig. 13 The transition to the swing phase of the left foreleg (LF) is prevented due to a perturbation decreasing the rolling motion amplitude (a force of 4 N is applied at t_{LH} with walking pattern (LG)). In this case, the transition is only temporary prevented and takes place during the next walking cycle. However, the timing of the onset of the left foreleg swing phase differs from the usual one (it occurs before the onset of the left hind leg swing phase). As a result, the model is destabilized and falls on the side

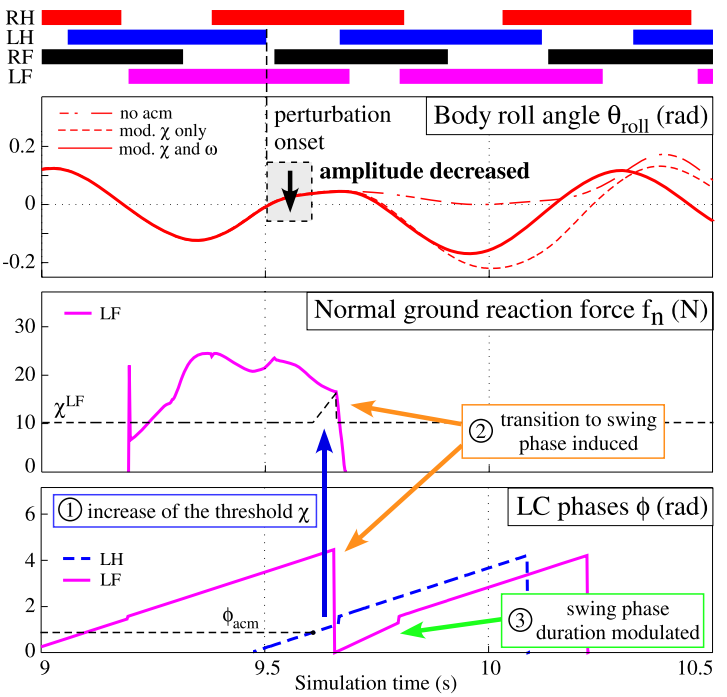

Fig. 14 Action of the ascending coordination mechanism and recovery from a perturbation decreasing the rolling motion amplitude (a force of 7 N is applied at t_{LH} with walking pattern (LG)). The increase of χ^{LF} triggers the transition from stance to swing. This restarts the oscillation of the body roll angle (shown by the difference between curves "mod. χ only" and "no acm"). Swing phase duration is subsequently shortened to reduce the increase of the roll angle (as it can be seen when comparing curves "mod. χ and ω" and "mod. χ only")

kinds of uneven terrains (elevated steps and slopes, as represented in Fig. 15) were evaluated. For the elevated steps, three situations were considered: the model steps once on an elevated step with its right hind leg (*hind leg on step* case), with its right foreleg (*foreleg on step* case) or has to continuously walk with both its right legs on a lateral step (*lateral step* case). To prevent the model to stumble on the steps, their borders were rounded off. For the slopes, both uphill walking (*up slope* case) and downhill walking (*down slope* case) were considered. In each simulation, the obstacle was positioned in such a way that the model had already reached its steady state before dealing with it. We found that the results are independent of the position of the obstacles with respect to the starting point of the robot.

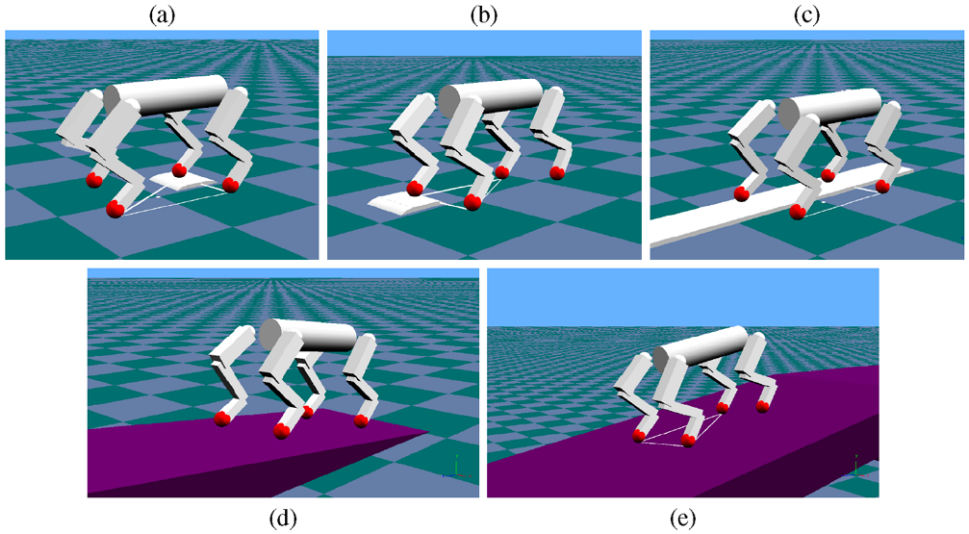

Fig. 15 Types of uneven terrain: (**a**) hind leg on step, (**b**) foreleg on step, (**c**) lateral step, (**d**) up slope, (**e**) down slope

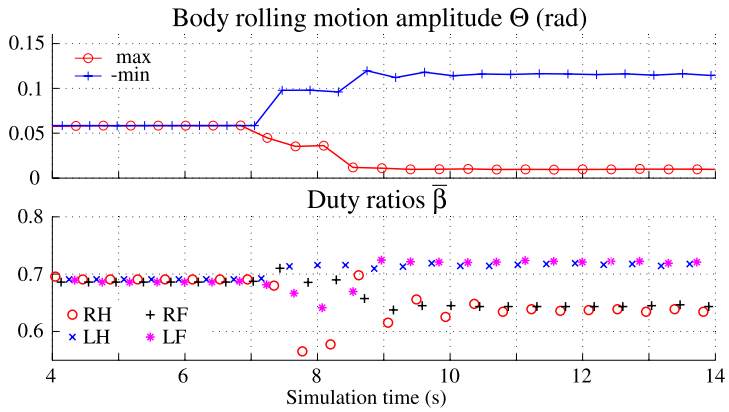

Fig. 16 Lateral step (4 mm) with (SH) walking pattern without ACM. When the simulation model is walking on the lateral step ($t \geq 7$ s), the rolling motion becomes asymmetric due to the perturbation (the minimum value is greater than the maximum, hence the model is leaning on the left) and the duty ratios are automatically adjusted (increased for the left legs and decreased for the right legs). As a result, a stabilizing moment is generated that counters the moment induced by the tonic perturbation. A new equilibrium is reached and the motion can be performed with a shifted mean value of the roll angle

Results The results are summarized in Table 6, which gives the maximum height of the step or the maximum inclination of the slope that the model could handle without falling. In the case of the lateral step, the inclination of the lateral slope equivalent to the step (when taking into account the width of the model) is also given. The control system, including the ACM, is able cope with medium level of terrain irregularity, such as steps in the range from 1 to 2 cm and slopes with inclinations of around 10° in the sagittal plane and of around 5° in the frontal plane, with both walking patterns. This shows that the control system is able to withstand not only punctual perturbations (like the lateral perturbation or walking once on a step) but also prolongated perturbations in the sagittal and frontal planes.

When dealing with terrain irregularities inducing perturbations in the lateral plane, the posture is stabilized by the automatic adjustments of the duty ratios (as shown in Fig. 16). The ascending coordination mechanism greatly improves the performances in situations where walking on the unevenness of the terrain causes a sudden decrease of

Table 6 Performances on uneven terrain. (a)∼(e) correspond to the types of uneven terrains shown in Fig. 15

Perturbation type	(SH)		(LG)	
	Without	With	Without	With
(a) Hind leg on step	5 mm	20 mm	12 mm	20 mm
(b) Foreleg on step	16 mm	16 mm	9 mm	10 mm
(c) Lateral step	4 mm	14 mm	6 mm	10 mm
(equivalent slope)	(1.9°)	(6.7°)	(2.9°)	(4.8°)
(d) Up slope	10°	10°	8°	8°
(e) Down slope	−6°	−12°	−9°	−10°

the rolling motion amplitude (*hind leg on step*) or the increase of the average load supported by one (*lateral step*) or both (*down slope*) forelegs. This is especially true for (SH), where the rolling motion amplitude is smaller than for (LG). On the other hand, (SH) performs better than (LG) in situations where the unevenness of the terrain causes an increase of the rolling motion amplitude (*foreleg on step*, *lateral step* after the addition of the ACM and *up slope*).

6 Discussion

6.1 Ascending coordination mechanism

Regarding the structure of the control system, an ascending excitatory connection linking the hind and foreleg leg controllers was required (Sect. 4.3). Interestingly, a similar mechanism seems to exist in animals as well. Results obtained by Akay et al. (2006) during cat locomotion on a transversely-split treadmill suggest the existence of an ascending excitatory pathway linking the systems generating flexor bursts in a foreleg and the ipsilateral hind leg. Together with two other pathways, it allows to explain the asymmetric adaptations of the walking patterns in the fore- and hind legs observed when reducing the speed of either the front or the back treadmills.

6.2 Utilization of the embodiment to integrate posture and rhythmic motion controls

Dynamic walking was realized in a broad range of cyclic periods and speeds using a control system extremely simple and distributed. Despite this simplicity, good performances against various perturbations were demonstrated. This achievement relies on the proper exploitation of the embodiment for walking and in particular the relation between rhythmic pitching motions of the legs in the sagittal plane and the rolling motion in the frontal plane, which is apparent in the transfer of leg loading between the legs. As explained in this contribution, a single mechanism using local rules based on leg loading information allowed to successfully control both of these periodic phenomena, hence realizing a basic integration of posture and rhythmic motion controls.

6.3 Dependence on parameter adjustments

The main drawback of using an approach strongly relying on sensory feedback is that the performances of the system become more dependent on the mechanical properties of the body and on the way it interacts with the environment. Therefore, some parameters of our system at the level of the motor command generation (i.e. $\hat{\Delta}^i$ and $\hat{c}^i$) had to be adjusted when the walking patterns were modulated. This could complicate the implementation of the control method on other platforms, mechanically different from the simulation model, because appropriate parameter adjustments should be found again. However, this should likely be only a minor difficulty because the number of parameters to tune is quite limited and the value of γ^{ipsi} can be used as an indication to guide the tuning process so that parameter tuning could even be automatized.

In agreement with this view, preliminary experiments aiming at implementing the proposed control strategy on a real robot (which is globally similar to the model, but which presents differences in the length of the segments, the total mass, the moment of inertia, the friction at the joints, and so on), seems to indicate that the control method can be applied without serious trouble for small variations of the mechanical properties (Maufroy et al. 2010).

6.4 Adding the stepping reflex as the next improvement

During locomotion, there is always an upper limit over which the stance period of a leg cannot be extended. It is ultimately given by the maximum stride length that can be realized given the physical limitation of the body and decreases as the speed increases. As the posture stabilization mechanism explained in Sect. 5.2.1 relies on the adjustment of the stance phase duration, the resistance ability of the control system against perturbations was found to decrease with the speed. In addition, there is also an absolute upper limit to the intensity of lateral perturbation that the system can withstand. If the projection of the center of mass goes beyond the line formed by the feet of the supporting legs (for example the left legs in the case of the perturbation used in Sect. 5.2), there is no way for the system to recover.

Hence, to overcome this limitations, a general legged locomotion controller should implement, in addition to the phase modulations which affect the current stance phase of a leg, other stabilization mechanisms that are able to influence its next stance phase. These include for example the stepping reflex, which adjusts the touchdown angle of the swinging legs using vestibular information. In animals, a similar mechanism contributes to the stabilization of the posture in the frontal plane via hip abduction and adduction movements (Misiaszek 2006; Karayannidou et al. 2009). We intend to consider this issue in the future and investigate the relative contributions of the phase-modulations-based and stepping-reflex-based stabilization mechanisms in more detail. However, we believe that phase modulations based on leg loading/unloading is a fundamental mechanism, contributing to posture control but also interleg coordination, and that it would give redundant and robust functions when adding the stepping reflex.

7 Conclusions and future works

Although Tekken2 (Kimura et al. 2007; Kimura and Fukuoka 2004) and BigDog (Boston Dynamics 2005) succeeded to realize adaptive dynamic walking in outdoor environment, still a lot of endeavors are required to develop a general legged locomotion controller with the ability to integrate both posture and rhythmic motion controls and shift continuously from one control method to the other according to locomotion speed. In this paper, we intended to show the basis of such controller, using a control architecture and a mechanical model as simple as possible.

Although the legs had no roll joint, rolling motion was still induced by the inverted pendulum motion during the two-legged stance phases. The rhythmic motion of each leg in the sagittal plane was generated by a single leg controller implementing phase modulations based on leg loading (to control the swing-to-stance transition) and unloading (to control the stance-to-swing transition). As local leg loading/unloading information reflects both the current phasic state of a leg (swing or stance) and the global posture of the body, our approach allowed to simultaneously coordinate the rhythmic motion of the legs in the sagittal plane and control the posture of the body in the frontal plane. As a result, coordination of the rhythmic motion of the legs (resulting in a gait) emerged, even without explicit coordination amongst the leg controllers, allowing to realize dynamic walking in the low- to medium-speed range. We showed that the proposed method has resistance ability against lateral perturbations to some extent, but that an additional ascending coordination mechanism between ipsilateral legs was necessary to withstand perturbations decreasing the rolling motion amplitude. Even without stepping reflex using vestibular information, our control system enabled low speed dynamic walking with long cyclic period and on uneven terrain, which was not realized in our former studies. Consequently, rhythmic motion control (including interleg coordination) and its integration with posture control were achieved while utilizing the body dynamics and the characteristics of legged locomotion under a gravity field.

Future work will be devoted to the implementation of our control system on a real robot (and the engineering challenges related to this topic) in order to show that the proposed leg controllers is an appropriate model of CPG in four-legged mammals. Promising results were obtained during preliminary experiments with a newly built quadruped robot, similar to the simulation model. We intend to pursue these experiments in order to compare simulation and experimental results.

Acknowledgements This work has been partially supported by a Grant-in-Aid for Scientific Research on Priority Areas "Emergence of Adaptive Motor Function through Interaction among Body, Brain and Environment" from the Japanese Ministry of Education, Culture, Sports, Science and Technology.

Appendix: Constant parameters of a leg controller and ACM

Table 7 Values of the constant parameters of LC and ACM

Leg controller				
$\hat{H}$	(m)	0.18		
$\hat{L}$	(m)	0.10		
$\hat{\chi}$	(N)	10		
		Hip	Knee	Ankle
$\hat{K}_{Pj,st}$	(Nm)	40	10	5
$\hat{K}_{Pj,sw}$	(Nm)	20	5	2.5
$\hat{K}_{Dj,st}$	(Nms)	0.56	0.28	0.20
$\hat{K}_{Dj,sw}$	(Nms)	0.40	0.20	0.14
ACM				
$\hat{\chi}_{ampl}$	(N)			15

References

Akay, T., McVea, D. A., Tachibana, A., & Pearson, K. G. (2006). Coordination of fore and hind leg stepping in cats on a transversely-split treadmill. *Experimental Brain Research*, *175*, 211–222.

Alexander, R. M. (1984). The gaits of bipedal and quadrupedal animals. *International Journal of Robotics Research*, *6*(3), 49–59.

Alexander, R. M. (1992). *Exploring biomechanics*. New York: Freeman.

Aoi, S., & Tsuchiya, K. (2005). Locomotion control of a biped robot using nonlinear oscillators. *Autonomous Robots*, *19*(3), 219–232.

Aoi, S., & Tsuchiya, K. (2006). Stability analysis of a simple walking model driven by an oscillator with a phase reset using sensory feedback. *IEEE Transactions on Robotics*, *22*(2), 391–397.

Berns, K., Ilg, W., Deck, M., Albiez, J., & Dillmann, R. (1999). Mechanical construction and computer architecture of the four legged walking machine BISAM. *IEEE/ASM Transactions on Mechatronics*, *4*(1), 32–38.

Boston Dynamics (2005). BigDog project. http://www.bdi.com/content/sec.php?section=BigDog.

Buchli, J., & Ijspeert, A. J. (2008). Self-organized adaptive legged locomotion in a compliant quadruped robot. *Autonomous Robots*, *25*(4), 331–347.

Cruse, H. (2002). The functional sense of central oscillations in walking. *Biological Cybernetics*, *86*, 271–280.

Deliagina, T., & Orlovsky, G. (2002). Comparative neurobiology of postural control. *Current Opinion in Neurobiology*, *12*, 652–657.

Duysens, J., & Pearson, K. G. (1980). Inhibition of flexor burst generation by loading ankle extensor muscles in walking cats. *Brain Research*, *187*, 321–332.

Ekeberg, O., & Pearson, K. (2005). Computer simulation of stepping in the hind legs of the cat: an examination of mechanisms regulating the stance-to-swing transition. *Journal of Neurophysiology*, *94*(6), 4256–4268.

Fukuoka, Y., Kimura, H., & Cohen, A. H. (2003). Adaptive dynamic walking of a quadruped robot on irregular terrain based on biological concepts. *International Journal of Robotics Research*, *22*(3–4), 187–202.

Grillner, S. (1981). Control of locomotion in bipeds, tetrapods and fish. In *Handbook of physiology II* (pp. 1179–1236). Bethesda: Am. Physiol. Soc.

Hildebrand, M. (1968). Symmetrical gaits of dogs in relation to body build. *Journal of Morphology*, *124*, 353–359.

Hirai, K., Hirose, M., Haikawa, Y., & Takenaka, T. (1998). The development of Honda humanoid robot. In *Proc. of ICRA 1998* (pp. 1321–1326).

Hobbelen, D. G., & Wisse, M. (2008). Controlling the walking speed in limit cycle walking. *International Journal of Robotics Research*, *27*(9), 989–1005.

Ijspeert, A. J. (2001). A connectionist central pattern generator for the aquatic and terrestrial gaits of a simulated salamander. *Biological Cybernetics*, *84*(5), 331–348.

Ijspeert, A. J. Crespi, A., Ryczko, D., & Cabelguen, J. M. (2007). From swimming to walking with a salamander robot driven by a spinal cord model. *Science*, *315*(5817), 1416–1420.

Jindrich, D. L., & Full, R. J. (2002). Dynamic stabilization of rapid hexapedal locomotion. *Journal of Experimental Biology*, *205*, 2803–2823.

Karayannidou, A., Zelenin, P. V., Orlovsky, G. N., Sirota, M. G., Beloozerova, I. N., & Deliagina, T. G. (2009). Maintenance of lateral stability during standing and walking in the cat. *Journal of Neurophysiology*, *101*, 8–19.

Kimura, H., Shimoyama, I., & Miura, H. (1990). Dynamics in the dynamic walk of a quadruped robot. *Advanced Robotics*, *4*(3), 283–301.

Kimura, H., Akiyama, S., & Sakurama, K. (1999). Realization of dynamic walking and running of the quadruped using neural oscillator. *Autonomous Robots*, *7*(3), 247–258.

Kimura, H., & Fukuoka, Y. (2004). Biologically inspired adaptive dynamic walking in outdoor environment using a self-contained quadruped robot: 'Tekken2'. In *Proc. IROS 2004* (pp. 986–991).

Kimura, H., Fukuoka, Y., & Cohen, A. H. (2007). Adaptive dynamic walking of a quadruped robot on natural ground based on biological concepts. *International Journal of Robotics Research*, *26*(5), 475–490.

Maufroy, C., Kimura, H., & Takase, K. (2008). Towards a general neural controller for quadrupedal locomotion. *Neural Networks*, *21*(4), 667–681.

Maufroy, C. (2009a). *Generation and stabilization of quadrupedal dynamic walk using phase modulations based on leg loading information*. Ph.D. dissertation, University of Electro-Communications (available at: http://robotics.mech.kit.ac.jp/kotetsu/Maufroy-phd-dissertation.pdf).

Maufroy, C., Kimura, H., & Takase, K. (2009b). Stable dynamic walking of a quadruped via phase modulations against small disturbances. In *Proc. of ICRA 2009* (pp. 4201–4206).

Maufroy, C., Nishikawa, T., & Kimura, H. (2010). Stable dynamic walking of a quadruped robot "Kotetsu" using phase modulations based on leg loading/unloading. In *Proc. of ICRA 2009* (accepted).

Misiaszek, J. (2006). Control of frontal plane motion of the hindlimbs in the unrestrained walking cat. *Journal Neurophysiology*, *96*, 1816–1828.

Miura, H., & Shimoyama, I. (1984). Dynamical walk of biped locomotion. *International Journal of Robotics Research*, *3*(2), 60–74.

Orlovsky, G. N., Deliagina, T. G. & Grillner, S. (1999). *Neural control of locomotion*. London: Oxford University Press.

Raibert, M. H. (1986). *Legged robots that balance*. Cambridge: MIT Press.

Righetti, L., & Ijspeert, A. (2008). Pattern generators with sensory feedback for the control of quadruped locomotion. In *Proc. of ICRA 2008* (pp. 819–824).

Rossignol, S. (1996) Neural control of stereoscopic leg movements. In L. B. Rowell & J. T. Sheperd (Eds.), *Handbook of physiology—exercise regulation and integration of multiple systems* (pp. 173–216). London: Oxford University Press.

Taga, G., Yamaguchi, Y., & Shimizu, H. (1991). Self-organized control of bipedal locomotion by neural oscillators. *Biological Cybernetics*, *65*, 147–159.

Taga, G. (1995). A model of the neuro-musculo-skeletal system for human locomotion II. Real-time adaptability under various constraints. *Biological Cybernetics*, *73*, 113–121.

Takanishi, A., Takeya, T., Karaki, H., & Kato, I. (1990). A control method for dynamic biped walking under unknown external force. In *Proc. of IROS 1990* (pp. 795–801).

Tomita, M. (1967). A study on the movement pattern of four limbs in walking. *Journal Anthropological Society of Nippon*, *75*, 120–146 171–194.

Tomita, N., & Yano, M. (2003). A model of learning free bipedal walking in indefinite environment—constraints self-emergence/self-satisfaction paradigm. In *Prof. SICE Annual Conf.* (pp. 3176–3181).

Tsujita, K., Tsuchiya, K., & Onat, A. (2001). Adaptive gait pattern control of a quadruped locomotion Robot. In *Proc. of IROS2001* (pp. 2318–2325).

Vukobratović, M., & Borovac, B. (2004). Zero-moment point—thirty five years of its life. *International Journal of Humanoid Robotics*, *1*(1), 157–173.

Yoneda, K., Iiyama, H., & Hirose, S. (1994). Sky-hook suspension control of a quadruped walking vehicle. In *Proc. of ICRA 1994* (pp. 999–1004).

Christophe Maufroy was born in Etterbeek, Belgium, on October 17, 1981. He received respectively the degrees of Ingenieur Civil Mecanicien and Ingenieur des Arts et Manufactures from the ULB (Universite Libre de Bruxelles, Brussels) and the ECP (Ecole Centrale Paris, Paris) in 2004, and a Ph.D. in engineering from the UEC (University of Electro-Communications, Tokyo) in March 2009. He is currently a researcher at the Division of Mechanical and System Engineering, Kyoto Institute of Technology, Kyoto, Japan. His research interest is related to the comprehension of how, in animals, simple and local control strategies result in the emergence of adaptive locomotion through the interactions between the nervous system, the body and the environment and how the principles underlying such emergent behaviors can be applied to robots. He is a member of the Robotics Society of Japan (RSJ).

Hiroshi Kimura was born in Hiroshima, Japan in 1961. He received the B.E., M.E., and Dr.E. degrees in mechanical engineering from the University of Tokyo, Tokyo, Japan, in 1983, 1985, and 1988, respectively. Currently, he is a Professor with the Graduate School of Science and Technology, Kyoto Institute of Technology, Kyoto, Japan. His research interests are the dynamics of legged locomotion robots and flapping robots.

Kunikatsu Takase received the B.E. degree in Mechanical Engineering from Yokohama National University in 1968, the M.E. degree from the University of Tokyo in 1970 and the Dr.E. from Tokyo Institute of Technology in 1986. He was with the Electrotechnical Laboratory (ETL) from 1970 to 1994. He has been a Professor of the Graduate School of Information Systems, University of Electro-Communications since 1994. His main research interests are in manipulation systems, network robotics, advanced teleoperation and autonomous robot control. He is a member of Robotics the Society of Japan, Society of Instrument and Control Engineers, Institute of Electrical Engineers of Japan, Virtual Reality Society of Japan, and Computer Society of the IEEE.